A SYSTEMATIC APPROACH TO OPTIMIZE THE COST OF CARBON INTEGRATION NETWORK

A Thesis

by

GIHONG KWAK

Submitted to the Office of Graduate and Professional Studies of
Texas A&M University
in partial fulfillment of the requirements for the degree of

MASTER OF SCIENCE

Chair of Committee,	Patrick Linke
Co-Chair of Committee,	Nimir Elbashir
Committee Member,	Hamid R. Parsaei
Head of Department,	Nazmul Karim

August 2016

Major Subject: Chemical Engineering

ABSTRACT

Carbon dioxide is a material which can be readily found in the atmosphere. However, as the amount of carbon dioxide from various man-made emission sources has been increasing steadily since the industrial revolution, anthropogenic carbon dioxide is placed in the highest portion in greenhouse gasses and threatens the climate with global warming. In the effort to reduce carbon dioxide emissions, many solutions were suggested. Among them, the construction of the Carbon Capture, Utilization and Storage (CCUS) system using carbon integration is the most attractive one because it is direct and efficient to suppress anthropogenic carbon dioxide emission.

However, since the current carbon integration network of the CCUS system requires capital investment and operating cost, it is necessary to minimize the total cost of the system. To achieve the minimum cost for the system, this work analyzed the cost components of the total cost and developed their linear least-cost models to achieve a rigorous global optimum solution. Then, these cost models were applied to previously developed carbon integration network formulations by substituting non-linear correlations available. This work illustrated the new approach to develop simple optimized cost models to minimize the total carbon integration cost for each carbon reduction target, and the carbon integration results with new cost models were obtained to propose the economic potential of the carbon integration network of the CCUS system.

DEDICATION

To my parents

ACKNOWLEDGEMENTS

First and foremost, I would like to express my deepest gratitude to my supervisor, Dr. Patrick Linke, for his kind guidance, professional insight, and endless support not only in this work but also in my entire graduate study. Without his support, this work would never be achieved.

I would like to thank Dr. Nimir Elbashir and Dr. Hamid Parsaei for the being co-chair and member of my thesis committee and for their valuable advice and time.

Moreover, I would sincerely appreciate to Dr. Sabla Al Nouri and Dhabia Al Mohannadi for their help and advises. Likewise, I also thank Raid Hassiba, Varun Chauhan, and Kholoud Abdulaziz. Also, I would like to thank fellow colleagues, CHEN faculties, and staffs.

I would like to thank Jeong-gu Kang and Seong-woo Ko for their kind advice and encouragement.

Last but not least, I would like to express my appreciation to my parents for their devotion and faith in me.

NOMENCLATURE

Per	Permeability
Diff	Diffusivity
Sol	Solubility
J	Gas permeance
δ	Thickness of membrane
F	Volumetric flow rate of permeate
A	Area of membrane
x	Volume fraction of a component in feed flow to the membrane
P_1	Feed pressure to membrane
y	Volume fraction of a component in permeance
P_2	Permeate pressure from membrane
y^{co2}	Volume fraction of CO_2
α	Selectivity for membrane
β	Pressure ratio for membrane
q_i *	Concentration of sorbate i
$\bar{q}$	Value of q averaged over an adsorbent particle
k_i^H	Henry constant
P_i	Pressure of sorbate i
S	Set of carbon sources
K	Set of carbon sinks

T	Set of carbon treatment technologies
R_s	Flow rate of raw source s
L_s	Lower limit flow of source s
M_s	Upper limit flow of source s
y_s	Composition of raw source s
$T_{s,k,t}$	Flow from source s to sink k treated with technology k
ε_t	Carbon removal efficiency of treatment technology t
y_s^u	Composition of raw source s
$L_{s,k}$	Lower limit flow of source-sink connection
$M_{s,k}$	Upper limit flow of source-sink connection
$X_{s,k}$	Binary for flow of the combined treated and untreated streams
γ_t	Amount of CO_2 emitted from the treatment unit energy use
$F^{CO2}{}_k$	CO_2 flow into the sink k
η_k	Sink efficiency
ε_p	Power consumption using carbon footprint
$C^{Treatment}{}_{s,k,t}$	Cost of treatment
$C^{Compressiont}{}_{s,k}$	Cost of compression
$C^{Transportation}{}_{s,k}$	Cost of transportation
$C^{Sinks}{}_k$	Cost of processing CO_2 in a given sink

$a_{s,k,t}$	Slope of a cost model for the treatment process
$b_{s,k,t}$	Intercept of the x-axis of a cost model for the treatment process
$C^{Transportation}{}_{s,k}$	Cost of transportation from untreated sources to sink
$c_{s,k}$	Slope of transportation model for untreated source
$d_{s,k}$	Intercept of the x-axis of transportation model for untreated source
$C^{Transportation}{}_{s,k,t}$	Cost of transportation from treated source to sink
$e_{s,k,t}$	Slope of transportation model for treated source
$f_{s,k,t}$	Intercept of x-axis of transportation model for treated source
Pc	Critical pressure
Vc	Critical molar volume
Tc	Critical temperature
ρc	Critical density
Zc	Compressibility in a critical point
Kij	Binary interaction parameter
ω	Acentric factor
P_{ini}	Pressure from the source
$\underline{V}$	Molar volume
R	Idea gas constant
Z	Compressibility
Z_{mix}	Compressibility of the mixture
y_c	Mole fraction of component c
Z_d	Compressibility of component d

a_{mix}	Value of a of the mixture
y_d	Mole fraction of component d
b_{mix}	Value of b of the mixture
b_c	Value of b of component c
k_{cd}	Binary interaction parameter of component c and d
I	Set of mass flow rates from source
J	Set of commercial pipe diameters
H	Set of number of compression stages
$C^{pipe}_{j,s,k}$	Capital cost of the pipe with diameter j from source s to sink k
Re	Reynolds number
ID_j	Internal diameter of the pipe diameter j
ρ	Density of the fluid
$u_{i,j}$	Velocity of the fluid with i th flow rate in pipe diameter j
μ	Viscosity of the fluid
M_i	i th Mass flow rate
A^p_j	Internal cross-sectional area of pipe diameter j
$f_{i,j}$	Friction factor with i th flow rate in pipe diameter j
ε	Surface roughness
$\Delta P_{i,j,s,k}$	Pressure drop with i th flow rate in pipe diameter j from source s to sink k
$L_{s,k}$	Distance between source s and sink k

$P^{trans}_{i, j, s, k}$	Pressure for the transportation with i th flow rate in pipe diameter j from source s to sink k
$W^{comp}_{i, j, s, k}$	Power consumption by compression with i th flow rate in pipe diameter j from source s to sink k
Z_h	Average compressibility of compression stage h
T_{in}	Temperature of the inlet
η_{is}	Isentropic efficiency
k_h	Specific heat ratio (C_p/C_v) of compression stage h
CR_h	Compression ratio with h of compression stages
$P^{cut\text{-}off}_{s,k}$	Cut-off pressure for source s to sink k
$W^{comp}_{i,s,k}$	Minimum power consumption for flow rate M_i
$W^{pump}_{i,j,s,k}$	Power consumption of pumping for flow rate M_i with pipe diameter j from source s to sink k
η_p	Pump efficiency
$CC^{cap}_{i,s,k}$	Capital cost for the compression for flow rate M_i from source s to sink k
$CC^{oper}_{i,s,k}$	Operating cost for the compression for flow rate M_i from source s to sink k
COE	Cost of electricity
$PC^{cap}_{i,s,k}$	Capital cost for the pump for flow rate M_i from source s to sink k
$PC^{oper}_{i,s,k}$	Operating cost for the pumping for flow rate M_i from source s to

	sink k
$TAC^{trans}_{i,j,s,k}$	Total annualized cost for flow rate M_i with pipe j from source s to sink k
m	Molar flow rate
$W_{comp'}$	Work done by the compression in the model from Hasan et al.
$CC_{comp'}$	Capital cost of the compression in the model from Hasan et al.
$CC_{operating'}$	Operating cost of the compression in the model from Hasan et al.

TABLE OF CONTENTS

Page

LIST OF FIGURES

Page

LIST OF TABLES

Page

1. INTRODUCTION

1.1 Carbon Dioxide

Carbon dioxide (CO_2) is available naturally in the atmosphere or a product after the combustion, and pure CO_2 is applied as a refrigerant or dry ice in our lives. The amount of CO_2 emission into the atmosphere had been stable due to the consumption of CO_2 in carbon cycle through the earth's ecosystem; however, since the industrial revolution in the eighteenth century, the emission of CO_2 into the atmosphere has been increasing steeply due to the growth of consumption of fossil fuel [1]. Now, anthropogenic CO_2 possesses the highest portion among greenhouse gasses and threatens the climate as the aspect of global warming [2], [3].

1.2 Carbon Dioxide Reduction Policies and Solutions

Reduction of anthropogenic CO_2 emission now became the critical issue of preventing global warming, and one hundred ninety-five countries agreed to invest toward decreasing the emission of CO_2 in Paris agreement in December 2015 [4]. Reflecting demand to reduce the emission of CO_2, many solutions were suggested to abate carbon emissions such as increasing energy efficiency, applying nuclear power or renewable energy instead of combusting fossil fuels, and adopting Carbon Capture and Storage (CCS) or Carbon Capture, Utilization and Storage (CCUS) [5].

Among these solutions, constructing carbon integration network to implement Carbon Capture, Utilization and Sequestration (CCUS) system emerged as one of a direct

and efficient method which suppress the anthropogenic CO_2 being released from stationary CO_2 emission sources into the atmosphere. CCUS is a system consisted of several components; CO_2 from emissions sources is captured and delivered via pipelines, ships or tank-lorries to sinks to store it underground permanently or utilize it for synthesizing into other material. Notably, economic benefit can be expected when proper sources match with profitable sinks such as oil reservoirs in the CCUS system [6]. Therefore, CCUS system can be constructed in carbon integration network for the optimum structure.

However, several obstacles are available to build the carbon integration network of CCUS system widely. First of all, some sources produce CO_2 with impurities such as sulfur oxide (SO_x), nitro oxide (NO_x) and nitrogen (N_2); these sources require appropriate purifying processes for this system while profitable sinks require a high concentration of CO_2 flow and impurities in the flow can decrease the transportation efficiency and cause environment or safety issue [7]. Additionally, the installation cost and operating cost of pipelines and compressors for connections from the carbon emission points to the profitable sinks should be considered prior to constructing the carbon integration network. Especially, since supercritical CO_2 is recommended for the delivery of CO_2 to the sink, compression cost can cause a high expenditure to operate the CCUS system. Lastly, only simple and limited connections between source and sink such as power plant to Enhanced Oil Recovery (EOR) oil reservoir are considered for the most profitable CCUS while this simple connection is not always available everywhere in the world. Also, since the Kyoto protocol's entry into the force from 2005 [4], European Union (EU), Australia, Japan,

South Korea and United States adopted carbon emission trading system, and this carbon trading system would lead the increase of interest regarding complex connections between multiple sources and sinks to establishing realistic carbon integration network of CCUS system.

1.3 Overview of the Thesis

The purpose of this work is to assess optimized source-sink matching under the carbon reduction target by establishing new CO_2 treatment and transportation cost models for currently available carbon integration network formulations of the CCUS system. Section two provides the literature review of CCUS system and its components, also offers basic idea regarding the carbon integration by means of the process optimization and mass exchange. Section three announces problem statement. Section four mentions the objective and scope of this work. Section five presents the problem formulation. Section six suggests optimization approaches to minimize the transportation cost of carbon dioxide, then the result of optimized transportation cost is provided. Section seven shows the minimizing the carbon dioxide treatment cost for the carbon integration network and its result. Finally, section eight presents the conclusions and recommendation for future work.

2. LITERATURE REVIEW

In this section, basic knowledge, previous work results regarding the CCUS system with its cost components are provided. And it also summarizes insights of the carbon integration and the process optimization to solve the problem with the systematic approach.

2.1 Cost Components of Carbon Capture, Utilization and Storage (CCUS)

Carbon Capture, Utilization and Storage (CCUS) system consists of carbon emission sources, CO_2 treatment processes, transportation processes of CO_2 and carbon sinks. To construct carbon integration network between available carbon emission sources and sinks, installing CO_2 treatment and transportation processes should be considered and capital investments and operating costs for these processes will be key factors for implementing carbon integration network. Thus, following part examines the currently developed technologies regarding transportation and treatment for the carbon integration network.

2.1.1 Transportation of Carbon Dioxide

The transportation of CO_2 plays an important role in the CCUS system while CO_2 emission sources are sited close or far from sinks, and this affects to the increase of carbon integration cost of CCUS system [8], [9]. Thus, both commercial and academic attempts focused on addressing the realistic expenditure for transportation of CO_2.

Many methods for estimating the cost of transportation of CO_2 have been announced while three phase options of gas, liquid and solid are available for delivery of CO_2. Commercially, sub-cooled liquid, supercritical or gaseous phase of CO_2 can be delivered using tanks, pipelines and ships. For the carbon integration network, since a large amount of CO_2 should be provided to the sinks, transportations using pipelines are preferred [10]. And liquid and supercritical phase of CO_2 are transported to the sinks rather than gaseous CO_2 while gas occupies a larger volume than liquid or supercritical phase and cause the increase of the cost. Techno-economic models based on the natural gas pipeline technologies are applied to the transportation of CO_2 [11]. These cost models are categorized as a Darcy-Weisbach-based model, mechanical energy balance model, mass flow rate calculation models and rule-of-thumb model depending on the method for computing pipe diameter [12]. McCollum et al. [13] well-documented cost models based on the natural gas pipeline, and it considered the pressure drop using Colebrook equation to compute the pipeline cost. Ghazi et al. [12] calculated diameters of pipelines based on the pressure drop from Darcy-Weisbach equation and established cost models by setting the thickness based on API 5L standard. Knoope et al. [11] presented the possibility of enhancement in cost models based on natural gas pipelines by considering the gaseous CO_2 transportation and various steel grade based on the thickness of pipeline from the calculation of maximum allowable operating pressure (MAOP) based on API standard [14]. Zhang et al. [15] compared sub-cooled CO_2 with supercritical CO_2 to optimize the pipeline transport of CO_2, and considered underground pipeline installation and the effect of heat exchange.

Nevertheless, all the models mentioned here show deviations from each other while all the factors considered in each work differs. Also, since these models are restricted to the transportation of pure CO_2 only, it is required to establish cost models for the CO_2 with impurities, and also to consider the transportation of CO_2 in the gaseous phase as mentioned in Knoope et al. [14].

2.1.2 Treatment Process to Capture Carbon Dioxide

Since the cost for treatment process to capture CO_2 from emission points dominates the total cost for implementing the CCUS system, many types of research were conducted to explore available treatment technology and select appropriate technology to make dilute CO_2 flow into concentrated one so that it can be utilized for profitable sources [10], [16], [17].

To capture CO_2, three capture systems are considered for commercial scale which are post-combustion capture system, oxy-fuel combustion system, and pre-combustion capture system. In the pre-combustion system, fuel is converted into carbon monoxide with hydrogen (this gas mixture refers to 'syngas') via reforming processes, and then hydrogen (H_2) is extracted by the shift reaction of carbon monoxide and water. CO_2 is selectively removed from the CO_2-H_2 mixture in the final stage. In oxy-fuel combustion system, a high concentration of oxygen separated from air separation unit is combusted with fuel and vapor consisted of carbon dioxide and water only are produced [10], [18]. Currently, since anthropogenic CO_2 is mainly emitted from combustion system such as power plants, the post-combustion capture system is considered as an attractive and

practical method. Treatment technologies in the post-combustion capture system are normally categorized into four areas; absorption, adsorption, gas separation membrane and cryogenic distillation. In this work, considering flow conditions of sources, only three options are selected; absorption, gas separation membrane and adsorption.

2.1.2.1 Absorption Technologies

In absorption technologies as its name implies, a solvent such as aqueous alkanolamine weakly bonds with hydrogen sulfide (H_2S) and CO_2 from a sour gas and this intermediate is regenerated via a reversible process by heating or pressurizing. Absorption technologies can be sorted as chemical and physical absorption depending on how solvent attach with H_2S and CO_2. Kidney et al. [19] presented comparisons between chemical and physical solvent as Table 1.

Table 1 Comparison between Chemical and Physical Absorption Technologies in Kidney et al. [19]

Technologies / Pros and Cons	Chemical absorption	Physical absorption
Pros	• Partial pressure of H_2S and CO_2 is not affecting • ppm levels of H_2S and CO_2 can be achieved	• Solvent regeneration consumes less energy than the one in chemical absorption • Solvent selectively reacts with H_2S or CO_2
Cons	• Solvent regeneration process is high energy intensive • Cannot selectively react with H_2S or CO_2	• Meeting the H_2S specification is difficult • Process is sensitive to acid gas partial pressure

Among the absorption technologies, chemical absorption has been applied since 1930 in natural gas processing [20]. Chemical absorption method using alkanolamine (hereafter amine) solvents, especially Monoethanolamine (MEA), are widely accepted to most CCUS system research while this technology is already implemented in industrial scale in the natural gas process and it can be operated with the flue gas with low CO_2 partial pressure.

In amine absorption depicted in Figure 1, amine reacts with CO_2 of flue gas in the absorber and forms chemical bond. The simple reaction scheme [21] is shown as following:

$$CO_2 \text{ absorption: } CO_2 + Solvent \rightarrow [Solvent/CO_2]_{complex}$$

The reacted amine is called rich-amine solution. The rich-amine solution then is transported to the stripper and heated by the reboiler. Heated rich-amine solution releases the CO_2 and becomes the lean-amine solution.

Solvent Regeneration: $[Solvent/CO_2]_{complex} + heat \rightarrow CO_2 + Solvent$

Lean-amine solution is now recycled and re-injected to the absorber.

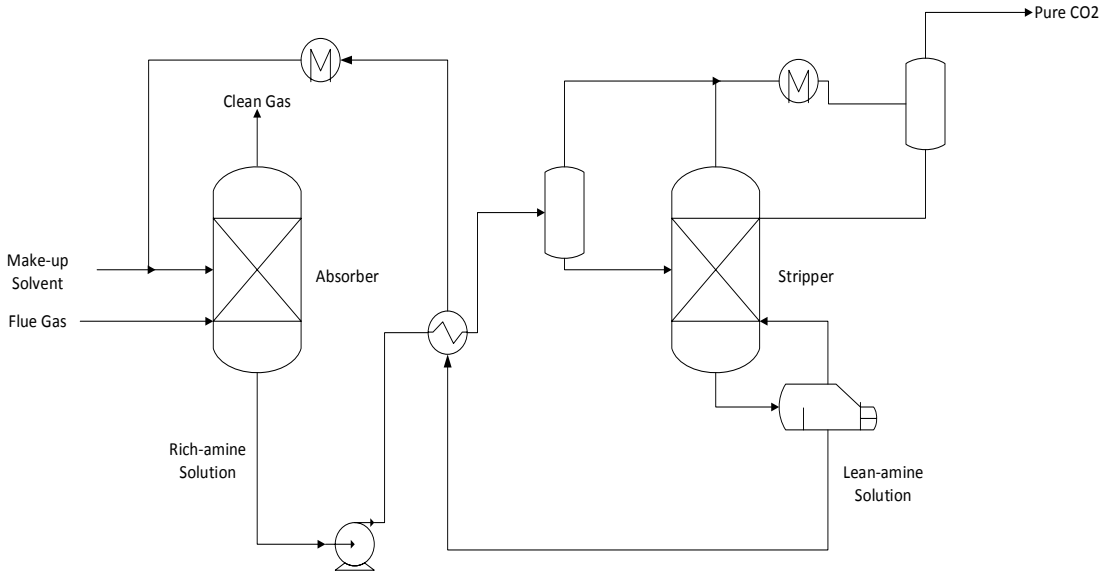

Figure 1 Process Flow Diagram of Amine Absorption from GPSA [20]

The advantage of amine absorption for capturing CO_2 is that it can be applied to retrofit existing stationary CO_2 emission sources [22]. Also, it is possible to obtain high recovery rate of CO_2 between 85~95% and purity of CO_2 in outlet up to 99% regardless low partial pressure of CO_2 in the flue gas [10]. However, amine absorption consumes energy to regenerate rich-amine solution into lean-amine solution, and degradation of

amine alarms the cost of continuous solvent make-up supplement and production of waste [23], [24]. To increase the thermal stability of MEA solvent, development of new solvent or mixing another type of alkanolamine are also considered [24], [25]. However, MEA is still preferred.

2.1.2.2 Gas Separation Membrane Technologies

Numerous researches on utilizing membrane technologies for recovering CO_2 from the flue gas are widely conducted. Two types of membrane technologies are mainly available for capturing CO_2; gas separation membranes and gas absorption membranes. Gas separation membrane technology is based on two mass transfer models; one is the pore model for porous membrane and the other is a solution-diffusion model [26]. Many works regarding gas separation membrane technologies adopt polymer membrane which is based on solution-diffusion model while it requires less spatial area, and can be operated flexibly. However, gas separation membrane requires a large area of membrane to handle low CO_2 concentration gas which can lead the increase of the treatment cost, and a significant amount of power consumption to create a driving force across the membrane for the separation [27].

To understand the gas separation membrane technology, solution-diffusion model is reviewed [28]. Permeability (Per) is the product of diffusion (Diff) and solubility (Sol) (equation (1)), and gas permeance (J) is the product of permeability and thickness of membrane (δ) (equation (2)). Applying Fick's law to equation (1) and (2) gives the equation (3) as following:

$$Per = Diff \times Sol \tag{1}$$

$$J = \frac{P}{\delta} \tag{2}$$

$$F = J \times A \times (xP_1 - yP_2) \tag{3}$$

where F: Volumetric flow rate of permeate, A: Membrane area, x: Volume fraction of a component in feed flow, P_1: Feed pressure, y: Volume fraction of a component in permeate, P_2: Permeate pressure.

If two components, such as CO_2-N_2, are only considered in the system, the volumetric flow (F) and the volume fraction of CO2 (y^{CO2}) as following:

$$F = J^{CO2}A(x^{CO2}P_1 - y^{CO2}P_2) + J^{N2}A[(1 - x^{CO2})P_1 - (1 - y^{CO2})P_2] \tag{4}$$

$$y^{CO2} = \frac{(\alpha - 1)(\beta x^{CO2} + 1) + \beta - \sqrt{(\alpha - 1)[(\beta x^{CO2} + 1) + \beta^2] - 4\alpha\beta x^{CO2}(\alpha - 1)}}{2(\alpha - 1)} \tag{5}$$

where α (selectivity): J^{CO2}/J^{N2}, β (pressure ratio): P_1/P_2.

Thus, if target volume fraction of permeate side, y^{CO2}, is set, two factors, selectivity and pressure ratio, play as process parameters. Not only selectivity and pressure ratio but also flow direction of each feed, residue and permeate also affect to in single gas separation membrane system. Additionally, it is possible to build multistage or cascade membrane system while single-stage membrane system cannot readily achieve over 85% of CO_2 purity [29], [30]. The simple two-stage membrane system is shown in Figure 2.

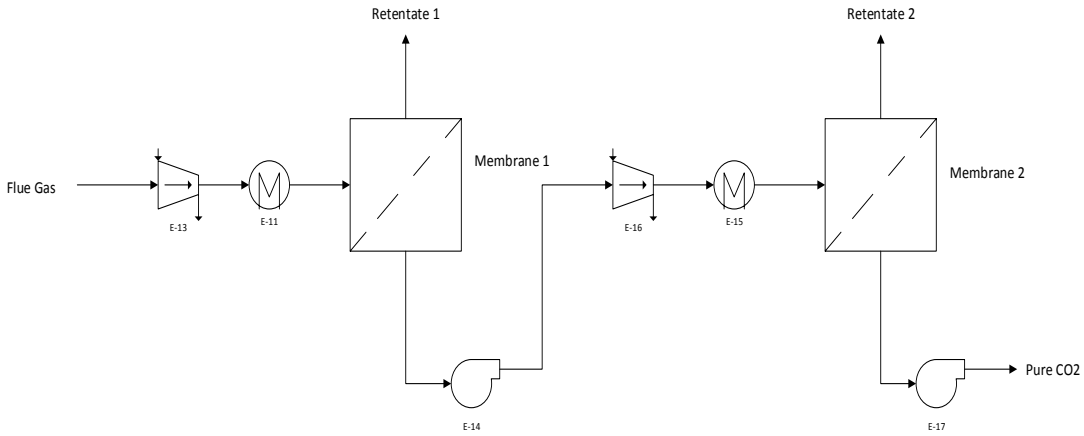

Figure 2 Scheme of Two-Stage Membrane System from Ho et al. [26]

To decide the optimal environment for the implementation of the gas separation membrane system in CCUS system, numerous works have been proposed. Merkel et al. [30] compared vacuum permeate with feed compression in a single stage and took account for advantages of the counter-flow module, then applied two-stage membranes to identify an optimal condition for 90% CO_2 capture. Zhai and Rubin [31] explored effects of feed-side pressure and CO_2 recycling under various CO_2 permeance. Shao et al. [28] presented the process optimization regarding minimum power requirement and CO_2 capture cost. Zhang et al. [27] evaluate the influences of membrane performance and membrane configurations by parametric study for a coal power plant. To achieve lower CO_2 capture cost, combination gas separation membrane technology and other treatment technologies are also considered. Scholes et al. [32] observed the effect of the combination of cryogenic distillation and three-stage membranes, and demonstrated that the capture cost is competitive with current amine absorption technology.

2.1.2.3 Adsorption Technologies

In adsorption process, a particular component in gas or liquid mixture selectively is attached on the surface of a solid adsorbent by weak Van der Waal's force or electron transfer; the former one is called physisorption and the latter one is called chemisorption. For the separation process, physisorption is preferred because it is economically viable for desorption and regeneration and chemisorption may not be reversible [33]–[35].

The adsorption process is based on mass transfer, and brief background knowledge regarding mass transfer is introduced for better understanding the adsorption process. Three mass transfer models are recognized for the adsorption which are 1) Instantaneous equilibrium model, 2) Pore diffusion model and 3) Linear driving force (LDF) model [33], [36], [37]. Among these three models, LDF model is widely applied while instantaneous equilibrium model neglects mass transfer resistances between gas and solid and pore diffusion model is limited to micro-pore diffusion. Also, LDF model can reduce the number of required boundary conditions [36].

$$Linear\ driving\ force\ (LDF)\ model\text{:}\ \frac{dq_i}{dt} = k_i(q_i^* - \bar{q}) \tag{6}$$

where q_i*: Concentration of sorbate i, $\bar{q}$: Value of q averaged over an adsorbent particle.

Diffusion by mass-transfer divided into two steps; first one is diffusion from bulk to the external surface of adsorbent, and the second one is internal diffusion. Mainly, adsorption process occurs during the internal diffusion and widely accepted three models for the adsorption is presented below;

$$\text{Henry's law: } q_i^* = k_i^H P_i \tag{7}$$

where q_i*: Concentration of sorbate i, k_i^H: Henry constant (vant Hoff eq.), P_i: Pressure of sorbate i.

$$\text{Langmuir isotherm: } q_i^* = \frac{q_i^s b_i P_i}{1 + \sum_j b_{1j} P_j} \tag{8}$$

where $q_i^s = k_i^1 + k_i^2 T$, $b_i = k_i^3 \exp(k_i^4/T)$.

$$\text{Freundlich isotherm: } q_i^* = q_i^s b_i P_i^{1/n} \tag{9}$$

Among these models, Langmuir isotherm or Freundlich isotherm models are frequently considered while the model of Henry's law is ideal one.

The adsorption process proceeds in sequential steps. These sequential steps are typically derived from Skarstrom cycle under atmosphere adsorption and Air Liquide cycle using vacuum desorption [36]. Skarstrom cycle with two packed adsorption column consists of pressurization, adsorption, counter-current blowdown and counter-current purge. During pressurization step, the first column with saturated with the adsorbate blows down to the atmosphere and second column is pressurized to a higher pressure than atmosphere pressure. In the adsorption step, high-pressure feed flow enters to the second column and particular component is attached to adsorbents; meanwhile, the first column purges the gas. After this step, first and the second column changes their role and act vice versa. Simple adsorption process system for carbon capture is presented as Figure 3.

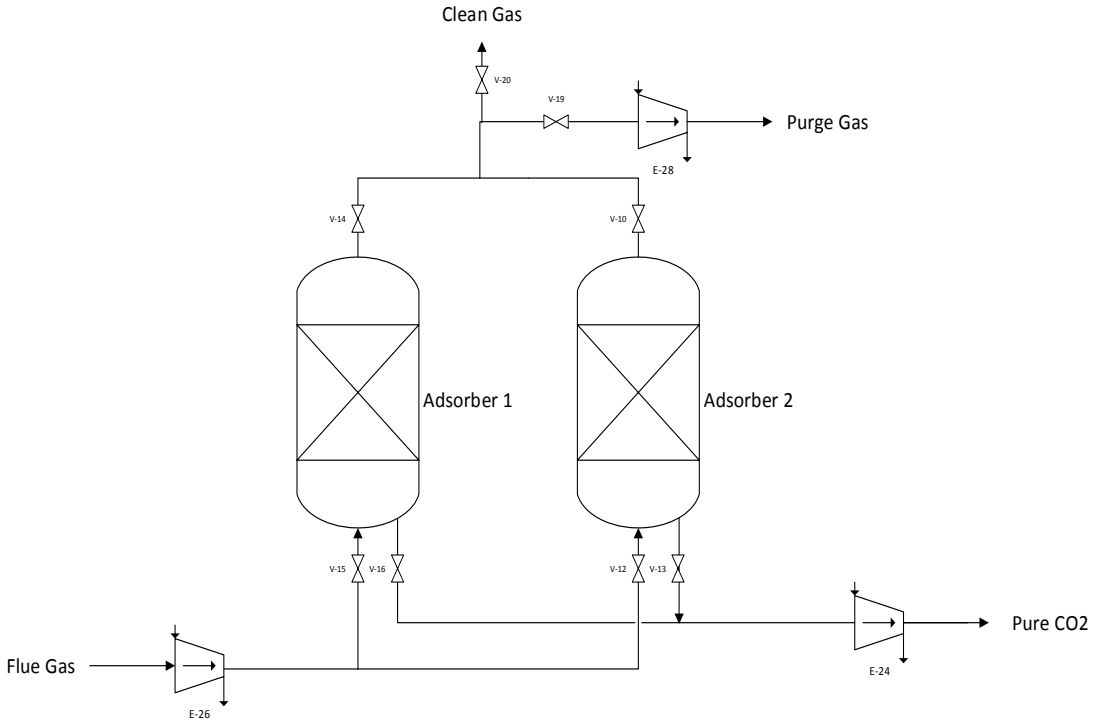

Figure 3 Scheme of PSA / VSA system from Ruthven et al. [36]

In adsorption process, using reversible nature of physical adsorption, absorbed species are released from adsorbents by heating or pressurizing adsorbent beds as introduced in the explanation of the Skarstrom cycle; thus, adsorbents can be recycled for further adsorption process; this process is called regeneration. In cyclic batch adsorption processes, methods of regeneration are the decisive factor for designing entire adsorption process. Four types of methods are widely accepted for the regeneration of adsorbents [34]; Thermal swing, pressure swing, purge gas stripping and displacement desorption. Among these regeneration methods, thermal swing using the hot gas stream and pressure swing by decreasing the pressure at constant temperature are generally applied while lower pressure or higher temperature can easily lead the desorption process [34], [38].

In CCUS system, adsorption process, which is currently applied to the hydrogen production process, can be considered as an alternative treatment technology instead of the chemical absorption while this process shows flexible operation, relatively low energy consumption and possibility of retrofitting to existing facilities. Specifically, possible benefits using pressure swing adsorption (PSA) and vacuum swing adsorption (VSA) technologies are investigated rather than temperature swing adsorption (TSA) while TSA requires large plant size [39]. Zhang et al. [39] compared PSA and VSA technology for carbon capture, and showed that feed gas temperature, outlet pressure and feed concentration of CO_2 affect to CO_2 capture cost. Also, VSA has more advantageous than PSA because it presents good recovery rate and purity of CO_2 with low electricity cost under certain conditions. Zhen et al. [40] simulated the VSA process with varying number of columns for adsorption and cycle configuration, and revealed that over 90% of purity cannot be achieved using only one column. Delgado et al. [41] investigated VSA process without rinse step to decrease the operating cost. However, adsorption technology using PSA or VSA depends on the vacuum or compression level to achieve a high purity of CO_2 which means the installation of multistage vacuum pumps or compressors may cause the increase both of the investment and operating cost [42].

2.2 Process Integration and Optimization for the CCUS System

Process integration (or process synthesis) is a systematic approach that produces better alternative process design based on incomplete information to meet certain objectives by revise the structure and parameters in the process [43], [44]. According to

El-Halwagi [44], optimization is one of effective method in process integration while it can suggest “best” solution among the set of possible solutions. The yardstick for the “best” solution can be judged under the circumstance of the objective function which indicates the maximization or minimization of a certain value.

Since CCUS system is consisted of carbon relocations from sources to sinks, the carbon integration, including both energy and mass integration simultaneously, for carbon footprint reduction, and optimum carbon allocations should be simultaneously considered for the realistic implementation of CCUS system. Mainly, two methods in the process system engineering are applied to the carbon integration which are 1) Graphical method and 2) Mathematic method. As the graphical methods in the direct-recycle network, material recycle pinch diagram and source-sink mapping diagram based on the lever-arm rule are widely used [44]. Diamante et al. [45], Ooi et al. [46] applied material recycle pinch diagram into CCUS system. Foo et al. [47] applied cascade analysis method for energy planning under carbon footprint limitation. While graphical methods mainly focus on the distribution of flow based on the component concentration, they cannot decide optimum allocation for achieving optimum cost under certain carbon footprint reduction target. In the mathematic model which is based on large sparse systems of equations, integer linear programming (ILP) model, nonlinear programming (NLP) model, or mixed-integer linear / non-linear programming (MILP / MINLP) are implemented by solving these models in branch-and-bound method or stochastic algorithms for CCS source-sink matching [48]. Zheng et al. [49] applied MINLP model for multi-objectives optimization for CCS source-sink matching while it only considers limited profitable sinks. He et al.

[48] implemented MILP model for optimal planning of CCS deployment under uncertainty while it is not aimed at the optimal cost for CCUS system. Middleton [50] introduced two-stage MILP optimization of energy network between anthropogenic CO_2 sources and EOR oil reservoirs by establishing piecewise linearization of cost models.

Al-Mohannadi and Linke [51] developed the carbon integration network models using MINLP formulations as shown in Table 2. Models from this work are consisted of 4 modules, which are the source, treatment (CO_2 separation), transportation and sink, as presented in Figure 4. The connection between each source and sink are expressed with overall mass balance and component mass balance which act as equality constraints. And lower / upper flow limit combined with non-negativity equations are set as the inequality constraints. Under these circumstances, minimization of summation of total expenditures of all modules and revenues from profitable sinks under the carbon reduction target shall be established as an objective function. The approach above is applied to the case study of Mesaieed Industrial City in Qatar while this case study has various carbon emitting sources and profitable sinks rather than oil reservoir, and showed the possibility of implementation of CCUS system into reality.

However, Al-Mohannadi and Linke [51] have complex cost correlations inside the MINLP formulations; this may cause robust solution and long computation time. And due to the parameters for the power consumption and amine absorption treatment cost, possibility to reduce the total carbon integration cost by optimizing these parameters is available.

Table 2 Carbon integration MINLP formulation of Al-Mohannadi and Linke [51]

	Formulations	Description
Source	1) Total Mass Balance $R_s = \sum_{k\in K}\sum_{t\in T} \varepsilon_t T_{s,k,t} + \sum_{k\in K} U_{s,k} \; ; \forall \; s \in S$ 2) Composition Mass Balance $R_s \times y_s = \sum_{k\in K}\sum_{t\in T} \varepsilon_t T_{s,k,t} y_{s,t} + \sum_{k\in K} U_{s,k} y_s^u \; ; \; \forall \; s \in S$ 3) Flow Rate Limit $L_s \leq R_s \leq M_s ; \forall \; s \in S$	$S=\{s\|s= 1,2,..,N_{sources}\}$: Set of carbon sources $K=\{k\|k=1,2,\ldots,N_{sinks}\}$: Set of carbon sinks $T=\{t\|t=1,2,\ldots,T_{max}\}$: Set of carbon treatment technologies R_s: Flow rate of raw source s L_s: Lower limit flow of source s M_s: Upper limit flow of source s y_s: Composition of raw source s $T_{s,k,t}$: Flow from source s to sink k treated with technology k ε_t: Carbon removal efficiency of treatment technology t y_s^u: Composition of raw source s $L_{s,k}$: Lower limit flow of source-sink connection $M_{s,k}$: Upper limit flow of source-sink connection $X_{s,k}$: Binary (0, 1) for flow of the combined treated and untreated streams γ_t: Amount of CO_2 emitted from the treatment unit energy use F^{CO2}_k: CO_2 flow into the sink k ηk: Sink efficiency ε_p: Power consumption using carbon footprint $C^{Treatment}_{s,k}$: Cost of treatment $C^{Compressiont}_{s,k}$: Cost of compression $C^{Transportation}_{s,k}$: Cost of transportation C^{Sinks}_{k}: Cost of processing CO_2 in a given sink
Sink	1) Total Mass Balance $F_k = \sum_{k\in K}\sum_{t\in T} T_{s,k,t} + \sum_{k\in K} U_{s,k} \; ; \forall \; k \in K$ 2) Composition Mass Balance $F_k \times Z_k^{min} \leq \sum_{k\in K}\sum_{t\in T} \varepsilon_t T_{s,k,t} y_{s,t} + \sum_{k\in K} U_{s,k} y_s^u \; ; \; \forall \; k \in K$ 3) $T_{s,k,t} \geq 0, y_{s,k,t} \geq 0 \; ; \; \forall \; s \in S, k \in K, t \in T$ $U_{s,k} \geq 0, y_{s,k} \geq 0 \; ; \; \forall \; s \in S, k \in K$	
Source-Sink Connection	1) $F_k \leq G_k^{max} \; ; \; \forall \; k \in K$ 2) $L_{s,k} X_{s,k} \leq T_{s,k,t} + U_{s,k} \leq M_{s,k} X_{s,k} ; \; \forall \; s \in S, k \in K, t \in T$	
Net Carbon Reduction Target (NCRT)	1) Net Capture $\geq$ NCRT 2) Net Capture $= \sum F_k^{CO2} (1 - \eta_k) - \sum T_{s,k,t} y_{s,t} \gamma_t - \sum F_k^{CO2} \varepsilon_p$	
Objective Function	$\text{Min} \sum_{s\in S}\sum_{k\in K} (C_{s,k}^{Treatment} + C_{s,k}^{Compression} + C_{s,k}^{Transportation} + C_k^{sinks})$	

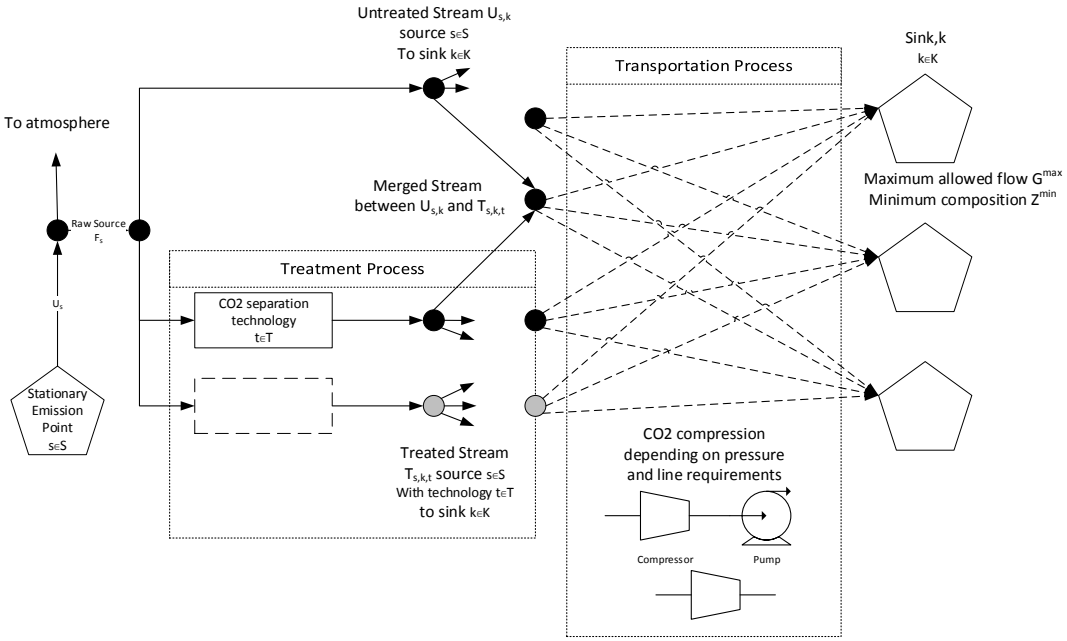

Figure 4 Graphical Scheme of Carbon Integration of Al-Mohannadi and Linke [51]

3. PROBLEM STATEMENT

As mentioned previously, Al-Mohannadi and Linke [51] have complexity among correlations inside as presented in Figure 5 and potential for being optimized for the transportation cost and adopted multiple carbon treatment options to decrease the carbon integration cost for the CCUS system.

To be more specific, firstly, since Al-Mohannadi and Linke [51] applied nonlinear cost correlations for calculating costs of compression, pumping and pipeline depending on the flow condition for each connection without considering optimal operating environment of each unit, it is possible to analyze the trade-off between pipeline cost and compression cost and reduce the cost of the transportation of CO_2 in the network by optimizing the units.

Secondly, although Al-Mohannadi and Linke [51] constructed the carbon integration network formulations using multiple CO_2 treatment technologies, it only applied the specific cost of the amine absorption technology for each source which has different composition and conditions. Thus, it is possible to apply various kinds of treatment technologies rather than applying only the amine absorption technology. Also, since the capital and operating cost for the treatment process depends on the scale of the process, treatment cost correlations depending on the flow rate under given circumstance should be considered.

Simultaneously MINLP models of Al-Mohannadi and Linke [51] can be simplified by applying linear transportation and treatment cost correlations to reduce the binaries and

other constraints; then MINLP models are converted to the MILP problem to solve the problem easily and fastly.

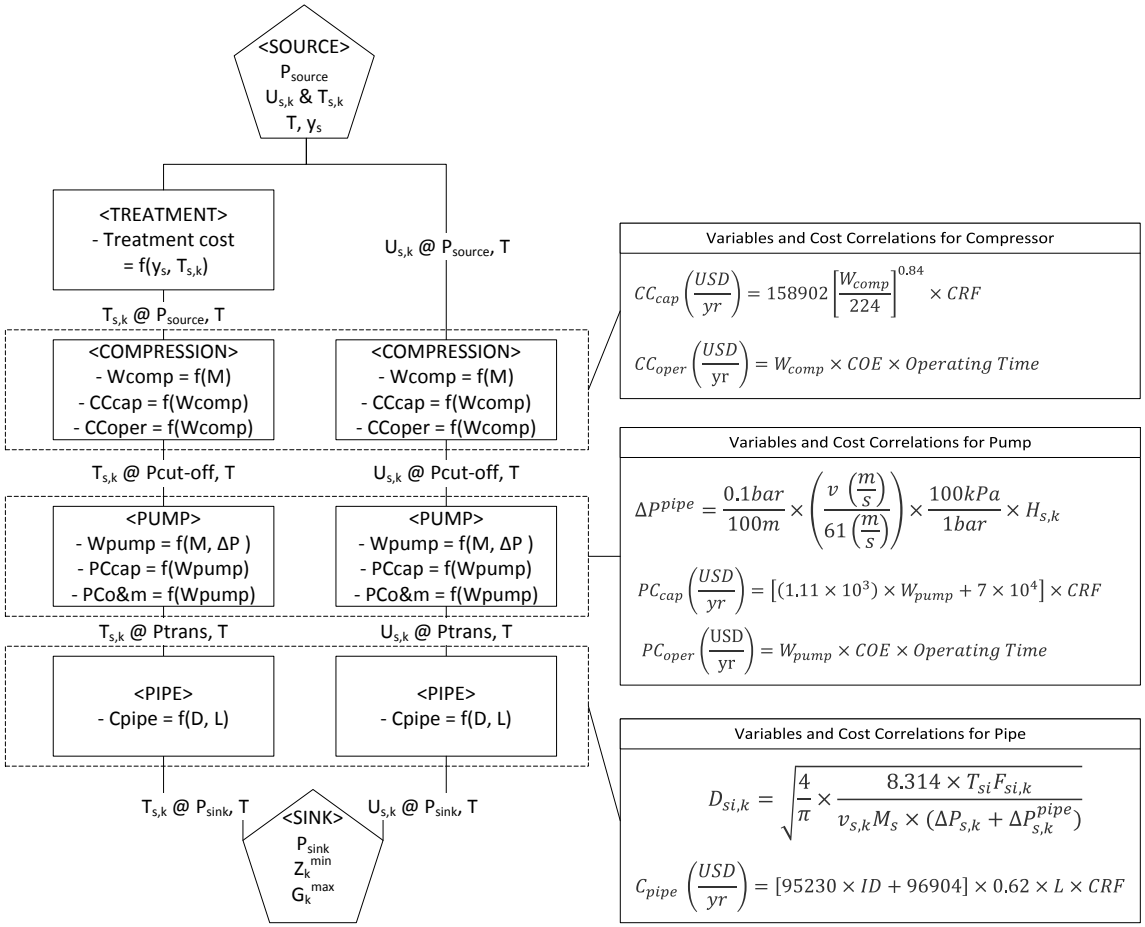

Figure 5 Cost Components and Correlations in Al-Mohannadi and Linke [51]

4. OBJECTIVE AND SCOPE

The main purpose of this work is to minimize the carbon integration cost in the CCUS system expressed in Al-Mohannadi and Linke [51]'s formulations by considering following work objectives:

- Modifying the objective function and cost components for adopting optimized cost components
- Achieving the optimized transportation cost by minimizing the trade-off between the compression and pipeline costs
- Adopting available cost models of various CO_2 capture technologies to decrease the cost of the treatment process
- Constructing linear cost correlations of transportation and treatment
- Applying newly developed simple cost correlations to previously developed carbon integration network problem for fast and rigorous globally optimized carbon integration cost

To achieve the objective of this work, this work will only focus on following:

- For the transportation cost of CO_2, optimizing the pipe diameter and the number of compression stages of each source-sink connection will be conducted. Other optimization work such as finding the optimum thickness of the pipe is not considered.

- For multiple treatment technologies, “black-box” linear cost models which can reflect the scale of economy and the composition of each emission source will be introduced based on the currently available work results.

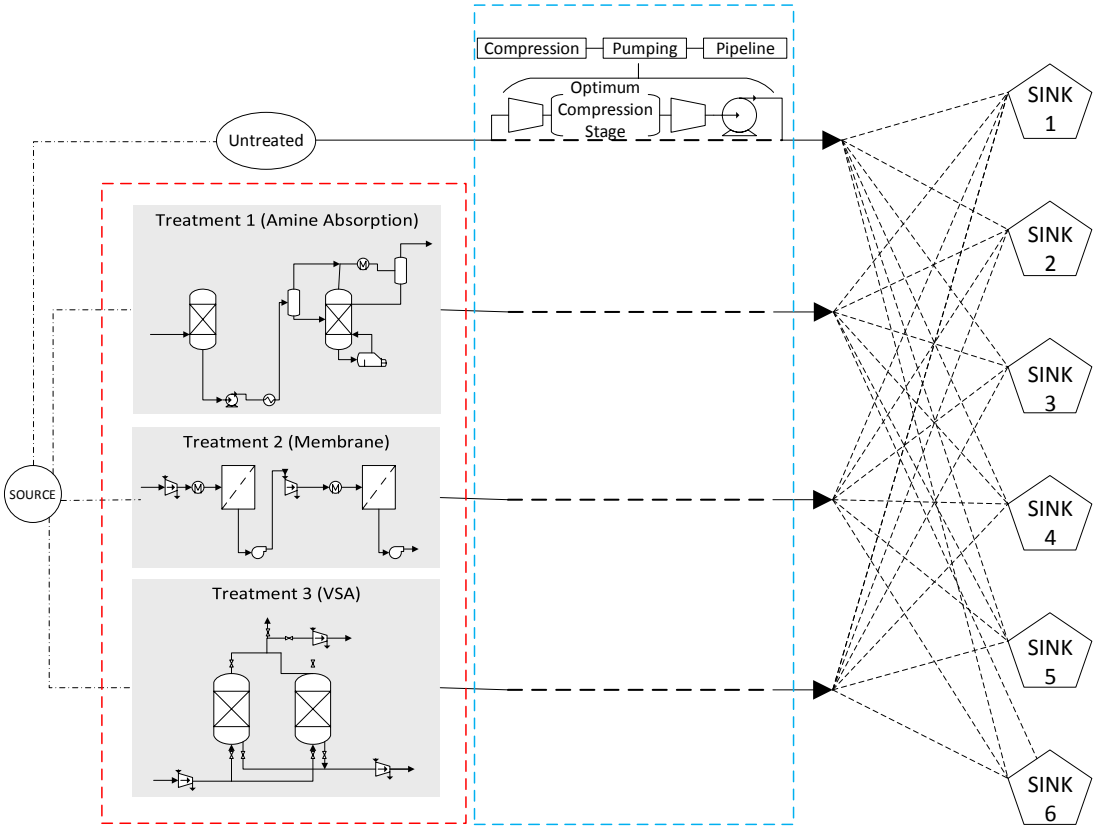

Figure 6 Graphical Scheme for the Scope of This Work

As the result of this work, globally optimized carbon integration network cost in the system would be announced with the optimal source-sink matching under specific carbon reduction target. Then, the benchmarking of carbon integration cost and the optimal source-sink matchings will be conducted between the result of this work and result

of Al-Mohannadi and Linke [51] to verify the improvement of the modification as shown in Figure 7.

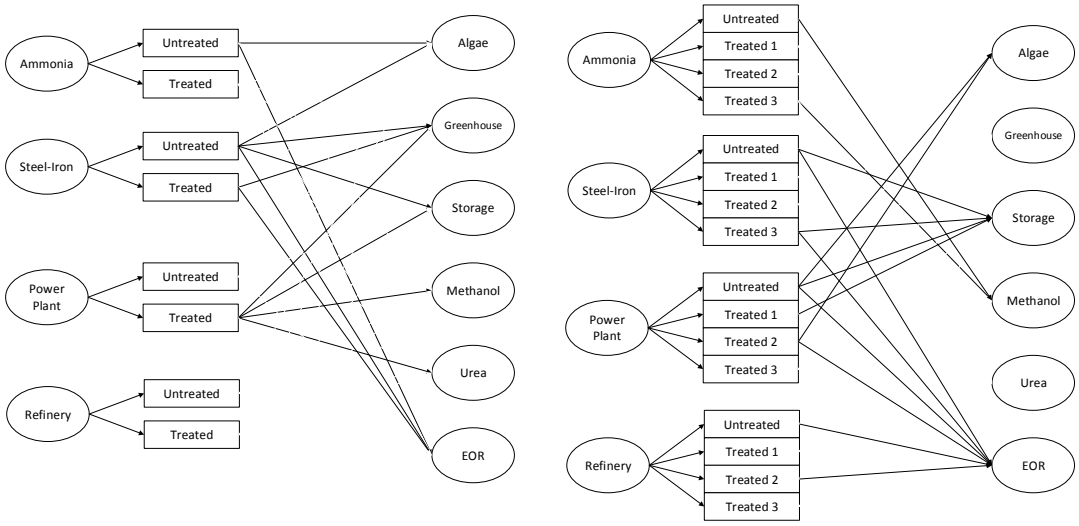

Figure 7 Examples of Optimal Carbon Source-Sink Matching Result (Left: Al-Mohannadi and Linke [51]'s Model, Right: Modified Model)

5. PROBLEM FORMULATION

In this section, new objective function and its cost components are announced to achieve an optimum carbon integration cost of the CCUS system. And cost models for the transportation and treatment of CO_2 are introduced separately. Mentioned in previous sections, to identify the transportation cost model, trade-off between pipeline cost and compression cost are investigated for every possible commercial pipe diameter and flow rate range, then cost models for the transport of CO_2 is established by linearization work. Regarding cost models for the treatment, cost models from Hasan et al. [52], [53] are applied by expanding them with possible composition and flow rate range and linearization.

The objective function is modified from the one from Al-Mohannadi and Linke [51] to consider the multiple treatments of CO_2, transportation of pure CO_2 flow and dilute CO_2 flow. And to apply the minimized transportation cost model, compression and pipeline cost models are merged. As the result, this work provided new objective function below:

$$\text{Min} \sum_{s\in S}\sum_{k\in K}\sum_{t\in T}(C_{s,k,t}^{Treatment} + C_{s,k}^{Transportation} + C_{s,k,t}^{Transportation} + C_{k}^{sinks}) \quad (10)$$

And simplified cost components for the transportation and treatment process are presented in Table 3.

Table 3 Cost Components and Cost Models

Cost Components	Cost Model	Description
$C^{Treatment}_{s,k,t}$ (USD/yr)	$C^{Treatment}_{s,k,t} = \sum_{s\in S}\sum_{t\in T}(a_{s,t}(\sum_{k\in K} X_{s,k,t} \times T_{s,k,t}) + b_{s,t})$ (11)	T={t|t=Chemical Absorption (ABS), Membrane Gas Separation (MEMB), Vacuum Swing Adsorption (VSA)}: set of carbon treatment technologies $a_{s,k,t}$, $b_{s,k,t}$: Linear regression coefficients of treatments Xs,t: Binary (0,1) for selecting treatment technology t
$C^{Transportation}_{s,k}$ (USD/yr)	$C^{Transportation}_{s,k} = \sum_{s\in S}\sum_{k\in K}(c_{s,k}U_{s,k} + d_{s,k})$ (12)	$C^{Transportation}_{s,k}$: Cost of transportation including compression from untreated sources to sink $c_{s,k}$, $d_{s,k}$: Linear regression coefficients of transportation economics for untreated source
$C^{Transportation}_{s,k,t}$ (USD/yr)	$C^{Transportation}_{s,k,t} = \sum_{s\in S}\sum_{k\in K}\sum_{t\in T}(e_{s,k,t}T_{s,k,t} + f_{s,k,t})$ (13)	$C^{Transportation}_{s,k,t}$: Cost of transportation including compression from treated source to sink $e_{s,k,t}$, $f_{s,k,t}$: Linear regression coefficients of transportation economics for treated source

6. COST MINIMIZATION OF CARBON TRANSPORTATION

In this section, steps for the minimizing the transportation cost of CO_2 in carbon integration network and their results based on the case study are presented. For the minimization steps, a set of optimal transportation costs for certain condition is collected, and this set of the minimum cost will be expressed in the function of the flow rate. And for each source-sink matching, this cost function will be substitute the complex cost correlations in Al-Mohannadi and Linke [51] to simplify formulations and achieve globally optimized cost of the carbon integration network of the CCUS system.

6.1 Establishment of Cost Models for the Transportation Process

In the work of Al-Mohannadi and Linke [51], each cost component is calculated using non-linear cost correlation. For instance, the cost of the compressor is proportional to the 0.84 root of the power consumption of the compressor, and the diameter of a pipeline which is used to calculate the pipeline cost is expressed in the square root of the pressure drop which can cause the complexity to solve.

This work explores the optimum point of pipeline, compression and pumping cost using brute force algorithm. Based on the optimization of compression stages and pipe diameter size under expanded fluid velocity range, linear cost models are derived and substituted non-linear correlations in the models of Al-Mohannadi and Linke [51]. This substitution work is expected to both simplify the optimization process and achieve cost-savings of transportation of CO_2 in the carbon integration network simultaneously.

To optimize the pipe diameter and compression stages for the linear cost model of one source-sink connection, following steps are conducted with twenty different flow rates which are step-wisely increased within the possible flow range based on the capacity of each source and each sink to obtain a trend-line of minimum total annualized transportation cost for one source-sink connection:

Step 1: Basic data acquisition and related method

- Set source and sink to get the information of each source and sink
- Adopt specific heat and compressibility values from Aspen Plus for the adiabatic compression
- Calculate average density applying Peng-Robinson (PR) equation of state (EOS) for the friction factor and pressure drop in the pipe

Step 2: Estimation of required pressure for the source-sink connection

- For every commercially available pipeline diameter, compute the friction factor
- Calculate the pressure drop and required pressure for the transportation
- Estimate each pipeline cost based on each diameter of the pipeline

Step 3: Calculation of power requirement for the compression and pumping

- Set the cut-off pressure of compression as the critical pressure of gas
- Calculate each compression power consumption for every possible compression stage in the range of allowed compression ratio range
- Select minimum power consumption among the required power of every case
- Consider the pump to increase the pressure of the liquid beyond cut-off pressure
- Compute the power consumption and the cost of the compressor and the pump

Step 4: Establishment of the linear transportation cost model for the transportation

- Under the acceptable fluid velocity, investigate the minimum total annualized cost of transportation for each case

- Plot the total annualized transportation cost versus the flow rate, and achieve a trend-line

- Establish the linear cost model for each connection, if necessary piecewise linearization work is conducted based on the value of root square of the cost model

To derive cost models using above steps, followings are assumed:

- Source

- Gas components: pure CO_2 and binary mixture of CO_2-N_2

- Outlet condition: 25℃ with dehydrated, desulfurized state

- Sink

- Required pressure should be satisfied by compression or pumping

- Pipeline and Compression

- Isothermal steady-state flow is assumed; thus, viscosity of the fluid is considered as a constant

- If fluid is delivered in gas phase, the density at 101 kPa, 313 K is applied, and if fluid is delivered in supercritical phase, the density at critical pressure, 313 K is applied

- Commercially available XS grade of pipe is applied to the pipeline [54]

- Allowable fluid velocity range is 5~30 m/s [55]

- Compression ratio range is from 1.5 to 6.0 [56]

- Compression stage: Maximum 10

- Miscellaneous

- Additional CO_2 emission by consuming electricity: 0.366kg CO_2 / kWh

- Cost of electricity (COE): 0.02 USD / kWh

- Capital recovery factor (CRF): 0.15

- Operating hours: 8760 hours/year

6.1.1 Acquisition of Basic Data for the Source-Sink Connection

In this part, basic information between source-sink will be set; then, thermodynamic properties for two process units, compression and pipe, will be acquired separately. Firstly, this work assumes that the compression process is adiabatic, and adopts specific heat and compressibility values from the properties analysis of Aspen Plus under the Peng-Robinson method. For the pipeline part, compressibility and density are only calculated to compute the friction factor and pressure drop while other properties are assumed as constants. Before estimating the density of the flue gas, each flue gas from each emission source is assumed as a binary gas mixture or pure CO_2 if it is treated, and fundamental thermodynamic properties of pure CO_2 and N_2 are adopted from the other literature [57]–[59] and announced in Table 4

Table 4 Basic Thermodynamic Properties of CO_2 and N_2

Components	Molecular Weight (MW, kg/kmol)	T_c (K)	P_c (kPa)	V_c (m^3/mol)	ρ_c (kg/m^3)	Z_c	ω	K_{ij}
CO_2	44.01	304.12	7376	94.07	469	0.274	0.225	-0.02
N_2	28.013	126.2	3394	0.0895	313	0.29	0.04	-0.02

Where P_c: Critical pressure (kPa), V_c: Critical molar volume, T_c: Critical temperature (K), ρ_c: Critical density (kg/m^3), Z_c: Compressibility in a critical point, K_{ij}: Binary interaction parameter, ω: Acentric factor.

To calculate the density of pure CO_2, [58]:

$$P_{ini} = \frac{RT}{\underline{V} - b} - \frac{a(T)}{\underline{V}(\underline{V} + b) + b(\underline{V} - b)} \tag{14}$$

$$a(T) = 0.45724 \frac{R^2 T_c^2}{P_c} \alpha(T) \tag{15}$$

$$\sqrt{\alpha} = 1 + \kappa \left(1 - \sqrt{\frac{T}{Tc}} \right) \tag{16}$$

$$\kappa = 0.37464 + 1.54226\omega - 0.26992\omega^2 \tag{17}$$

$$b = 0.07780 \frac{RT_c}{P_c} \tag{18}$$

where P_{ini}: Pressure from the source (kPa), V: Molar volume (m^3/kmol), T: Temperature (K), R: Idea gas constant (8.314 kJ / (kmol K)), Z: Compressibility.

Then Z = PV / RT relation is applied to above PR EOS with calculating the value of a and b based on initial source condition to express function of Z into polynomial equation,

$$Z^3 - (1 - B)Z^2 + (A - 3B^2 - 2B)Z - (AB - B^2 - B^3) = 0 \quad (19)$$

$$A = \frac{aP}{(RT)^2} \quad (20)$$

$$\mathrm{B} = \frac{\mathrm{bP}}{RT} \quad (21)$$

For the mixture of CO_2-N_2 mixture, mixing rules from Sandler [58] are applied as following:

$$Z_{mix}\left(T,\ P,\ \underline{y}\right) = \sum_{c=1}^{C} y_c Z_c(T,\ P) \quad (22)$$

$$a_{mix} = \sum_{c=1}^{C}\sum_{d=1}^{D} y_c y_d a_{cd} \quad (23)$$

$$b_{mix} = \sum_{c=1}^{C} y_c b_c \quad (24)$$

$$a_{cd} = \sqrt{a_{cc}a_{dd}}(1 - k_{cd}) = a_{dc} \quad (25)$$

where Z_{mix}: Compressibility of the mixture, y_c: Mole fraction of component c, Z_d: Compressibility of component d, a_{mix}: Value of a of the mixture, y_d: Mole fraction of component d, b_{mix}: Value of b of the mixture, b_c: Value of b of the component c, k_{cd}: Binary interaction parameter of component c and d.

Then the cubic equation of Z is solved using the Solver in Microsoft Excel®, and apply the relation of V = ZRT / P to calculate the density of the fluid using ρ = Molecular weight (MW) / V.

6.1.2 Estimation of the Required Pressure for the Transportation

From this section, brute force algorithm to calculate the properties for one source-sink connection is applied. Thus, to avoid the confusion, a number of sets as a basis for the iterating work for step 2 and 3 is defined:

S{s|s = 1, 2, 3, …, $N_{sources}$| S is a set of carbon sources}

K{k|k = 1, 2x, 3, …, N_{sinks}| K is a set of carbon sinks}

T{t|t = 1, 2, 3, …, T_{max}| T is a set of carbon treatment technologies}

I{i|i = 1, 2, 3, …, I_{max}| I is a set of mass flow rates from source}

J{j|j = 1, 2, 3, …, J_{max}| J is a set of commercial pipe diameters}

H{h|h = 1, 2, 3, …, H_{max}| H is a set of number of compression stages}

For every carbon steel pipeline with XS grade commercially available (37 types of nominal pipe diameters: 0.125 ~ 56 inches from ASME / ANSI B.36 [60]), internal diameter and area of each pipeline is calculated.

$$ID_j = Outer\ Diameter\ of\ pipe\ j - 2 \times thickness\ of\ pipe\ j \quad (26)$$

$$A_j^{pipe} = \frac{\pi}{4} \times ID_j \quad (27)$$

where ID_j: Internal diameter of pipe j (m), $A^{pipe}{}_{,j}$: Internal cross-sectional area of pipe j (m^2).

Also, each capital cost for each pipeline diameter is calculated using following cost model from Al-Mohannadi and Linke [51]:

$$C_{j,s,k}^{pipe} = [95230 \times Nominal\ Pipe\ Size, j + 96904] \times 0.62 \times L_{s,k} \times CRF \quad (28)$$

while $C^{pipe}_{j,s,k}$: Capital cost of the pipeline (USD/yr), 0.62: Conversion factor from kilometer to a mile (mile / km), $L_{s,k}$: Distance between source s to sink k (km), CRF: Capital recovery factor (0.15).

Reynolds number for flow rate M_i with pipe j ($Re_{i,j}$)is calculated using the information of internal diameter and the density value from the previous section:

$$\mathrm{Re}_{i,j} = \frac{ID_j \rho u_{i,j}}{\mu} \quad (29)$$

where ID_j: Internal diameter of the pipe j (m), ρ: Density of the fluid (kg/m^3), $u_{i,j}$: Velocity of the fluid for pipe j with i th flow rate (m/s), μ: Viscosity of the fluid (Pa.s).

Also, the fluid velocity ($u_{i,j}$) is computed using the relation below:

$$\mathrm{u}_{i,j} = \frac{M_i}{\rho A_j^{pipe}} \quad (30)$$

where M_i: i th mass flow rate (kg/s).

Calculated Reynolds number is assigned to calculate the friction factor ($f_{i,j}$) in the pipeline. To calculate the friction factor in the pipeline, Churchill equation is applied in this work [57]:

$$\frac{1}{\sqrt{f_{i,j}}} = -4\log\left[\frac{0.27\varepsilon}{ID_j} + \left(\frac{7}{Re_{i,j}}\right)^{0.9}\right] for\ turbulent\ flow\ (Re > 4000) \quad (31)$$

$$f_{i,j} = \frac{16}{Re_{i,j}}\ for\ laminar\ flow\ (Re \leq 4000): \quad (32)$$

where $f_{i,j}$: Friction factor for pipe j with flow rate M_i, ε: Surface roughness (0.0000457m [57]).

Then, pressure drop is calculated using the equation from Ghazi et al. [12]:

$$\Delta P_{i,j,s,k} = \frac{8 f_{i,j} L_{s,k} {M_i}^2}{\rho \pi^2 I D_j^5} \quad (33)$$

where $\Delta P_{i,j,s,k}$: Pressure drop with mass flow M_i and pipe j from source s to sink k (kPa).

After the computation of the pressure drop in the pipeline, pressure for the transportation with flow rate M_i and pipe j from source s to sink k ($P_{trans\ i,j,s,k}$) is defined as the sum of the required pressure for the sink and the pressure drop in the pipeline.

$$P_{i,j,s,k}^{trans} = P_{sink} - P_{source} + \Delta P_{i,j,s,k} \quad (34)$$

6.1.3 Calculation of Required Power of Compression and Pumping

To begin with calculating the power consumed by the compressor and pump, critical pressure of pure gas or gas mixture was set as cut-off pressure ($P^{cut\text{-}off}_{s,k}$) of compression and the range of compression ratio was set from 1.5 to 6.0. Then compression ratio (CR_h) is calculated as by increasing the number of compression stages (h) as following:

$$CR_h = \sqrt[h]{\frac{P_{s,k}^{cut-off}}{P_{source}}} \quad (35)$$

where CR_h : Compression ratio with h of compression stages.

If $P^{trans}_{i,j,s,k}$ exceeds the $P^{cut\text{-}off}_{s,k}$, installation of the pump will be considered while it has more economic benefit than installing a compressor. Then, the power consumption

for the compression and pumping is computed using the equations from McCollum et al. [13] as below:

$$W_{i,h,s,k}^{comp} = \left(\frac{M_i Z_h R T_{in}}{MW \times \eta_{is}}\right)\left(\frac{k_h}{k_h - 1}\right)\left[(CR_h)^{\frac{k_h-1}{k_h}} - 1\right] \quad (36)$$

where $W_{comp,\ h}$: Power consumption by compressor with compression stage h, T_{in}: Temperature of the inlet (K), MW: Molecular weight (kg/kmol), η_{is}: Isentropic efficiency (0.75), k_h: Specific heat ratio (C_p/C_v) for stage h, Z_h: Average compressibility of stage h.

The calculation of power for each compression stage adopted values of specific heat ratio and compressibility of Aspen Plus from Step 1. After calculating the total power consumption of each compression stage, the minimum power consumption for flow rate M_i ($W^{comp}_{i,s,k}$) is defined as following:

$$W_{i,s,k}^{comp} = minmum\left(W_{i,h,s,k}^{comp}\right), h \in H \quad (37)$$

$$W_{i,j,s,k}^{pump} = \left(\frac{M_i(P_{i,j,s,k}^{trans} - P_{s,k}^{cut-off})}{\rho_c \eta_p}\right) \quad (38)$$

where $W^{pump}_{i,j,s,k}$: Power consumption of pumping, η_p: Pump efficiency (0.75).

The capital and the operating cost models in Al-Mohannadi and Linke [51] were modified and applied to compare the result with the previous work:

$$CC_{i,s,k}^{cap} = 158902\left[\frac{W_{i,s,k}^{comp}}{224}\right]^{0.84} \times CRF \quad (39)$$

$$CC_{i,s,k}^{oper} = W_{i,s,k}^{comp} \times COE \times Operating\ Time \quad (40)$$

where $CC^{cap}_{i,s,k}$: Capital cost for the compression (USD/yr), $CC^{oper}_{i,s,k}$: Operating cost for the compression (USD/yr), COE: Cost of electricity (USD/kWh), Operating Time: 8760 (hr/yr).

$$PC_{i,j,s,k}^{cap} = \left[(1.11 \times 10^3) \times W_{i,j,s,k}^{pump} + 7 \times 10^4\right] \times CRF \quad (41)$$

$$PC_{i,j,s,k}^{oper} = W_{i,j,s,k}^{pump} \times COE \times Operating\ Time \quad (42)$$

where $PC^{cap}_{i,j,s,k}$: Capital cost for the pump (USD/yr), $PC^{oper}_{i,j,s,k}$: Operating cost for the pumping (USD/yr).

6.1.4 Establishment of Linear Cost Models for the Transportation

The total annualized cost for j th diameter pipe from source s to sink k with flow rates of M_i ($TAC^{trans}_{i,\ j,\ s,\ k}$) is defined as the summation of each capital cost of pipe j, compressor and pump, and operating cost of compression and pumping unit.

$$TAC_{i,j,s,k}^{trans}\left(\frac{USD}{yr}\right) = C_{i,j,s,k}^{pipe} + CC_{i,s,k}^{cap} + CC_{i,s,k}^{oper} + PC_{i,j,s,k}^{cap} + PC_{i,j,s,k}^{oper} \quad (43)$$

Then minimum $TAC^{trans}_{i,\ j,\ s,\ k}$ is selected under the allowed fluid velocity range and plotted by varying flow rates to establish the linear cost model and their coefficients $c_{s,k}$, $d_{s,k}$, $e_{s,k,t}$ and $f_{s,k,t}$ for the source-sink connection. If the value of R^2 of the cost model is less than 0.9, piecewise linearization work is conducted to increase the accuracy of the cost model.

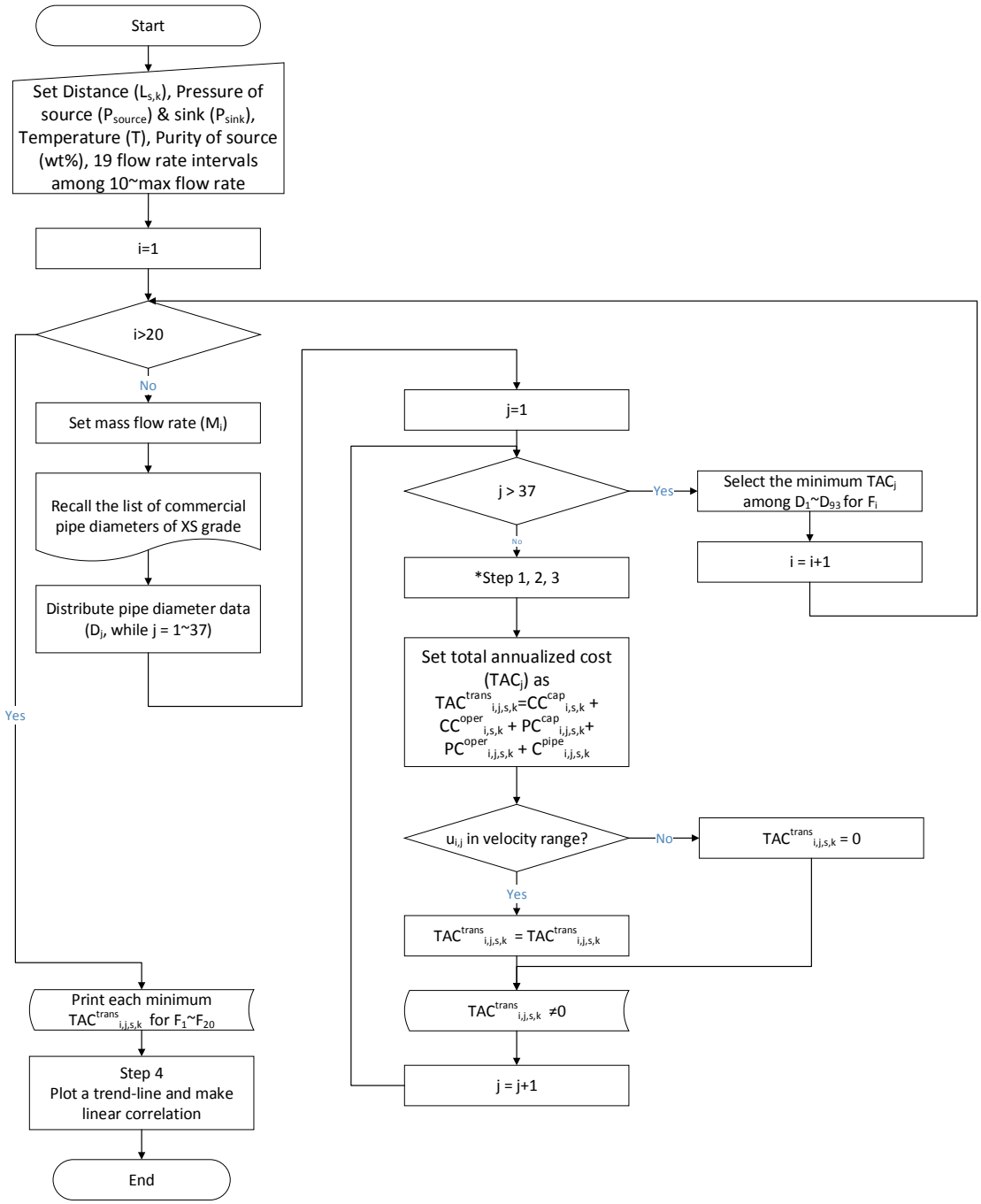

Figure 8 Flow Diagram of Linear Total Annualized Transportation Cost Models for One Source-Sink Connection

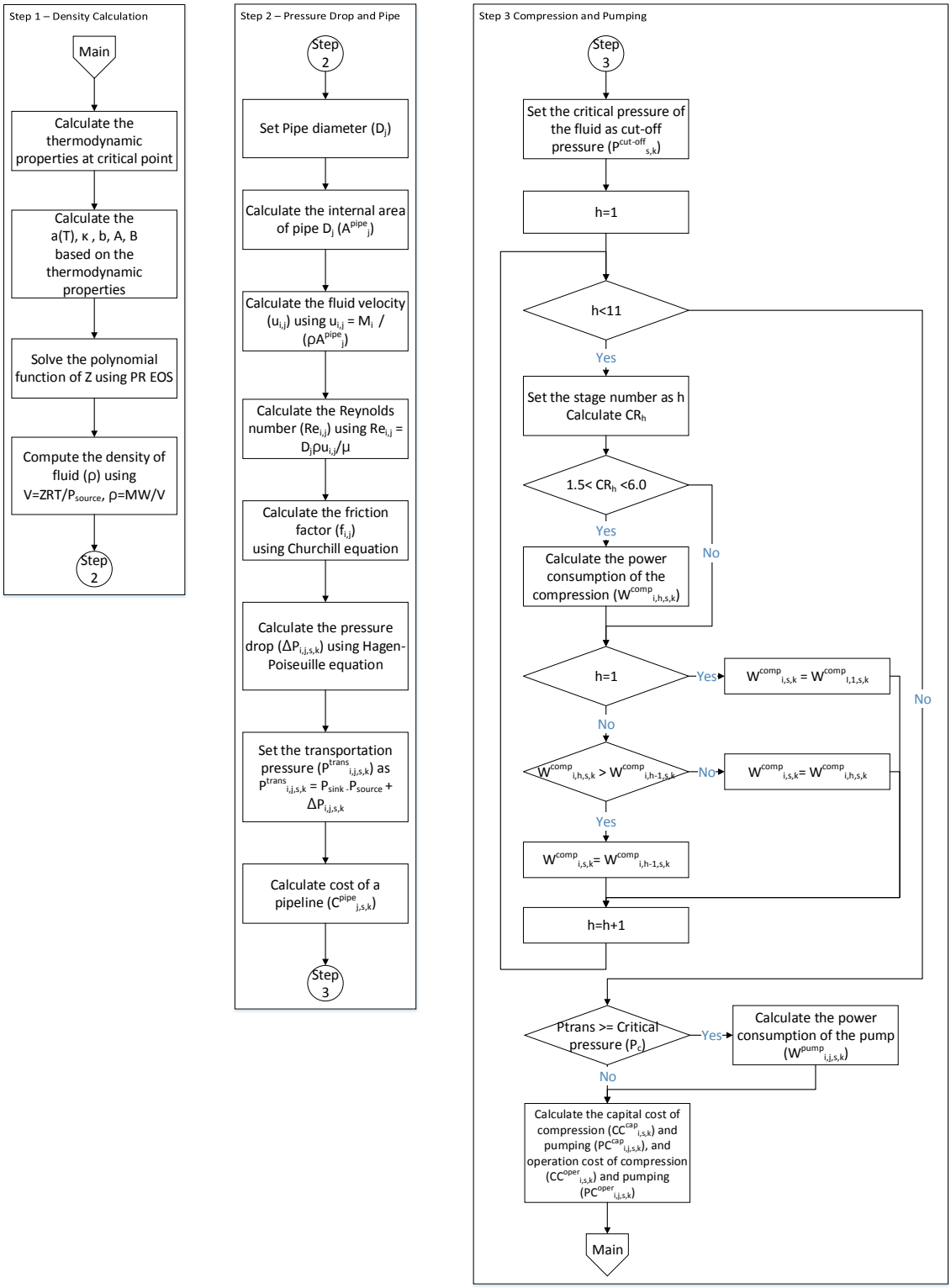

Figure 9 Subroutine Flow Diagrams of Step 1, 2 and 3 for Main Flow Diagram

6.2 Cost Models of the Transportation Process for the Case Study

Prior to deriving the cost models for the transportation, the temperature from each source was set to 298 K, and pressure from each source is set to 101kPa. The effect of pressure to viscosity of CO2 is investigated, and Fenghour et al. [61] showed the relationship that the pressure barely affects to the viscosity: Thus, viscosity set as a constant in this work. The information of sources and sinks from Al-Mohannadi and Linke [51] are presented in Table 5, Table 6 and Table 7 .

Table 5 CO_2 Emission Source Information from Al-Mohannadi and Linke [51]

Source	Stream	CO_2 (wt%, dry)	N_2 (wt%, dry)	ρ dry (kg/㎥)	CO_2 Flow, (MTPD)
Fertilizer Complex	Ammonia (NH_3) Plant	100	0	1.85	977
Steel Production	Iron mill	44	56	0.97	3451
Natural gas power plant	Post-combustion flue gas	7	93	0.74	9385
Refinery	Boiler	27	73	0.81	1092

Table 6 CO2 Sinks Information from Al-Mohannadi and Linke [51]

Sink	CO_2 composition (wt%)	Flow CO_2 (MTPD)	P, (kPa)	C_k^{sink} (USD/t CO_2)	η_k
Algae	6	283	101	0	0.42
Greenhouses	94	1030	101	-5	0.5
Methanol Plant	99.9	1710	8080	-21	0.098
Urea Plant	99.9	1126	14140	-15	0.39
EOR	94	2739	15198	-30	0
Saline storage	94	8317	15198	8.6	0

Table 7 Distance between Sources and Sinks from Al-Mohannadi and Linke [51]

Source / Sink (km)	Algae	Greenhouse	Saline Storage	Methanol Plant	Urea Plant	EOR
Ammonia Plant	1.72	25.38	1.51	1.51	1.55	1.56
Steel	2.07	25.73	1.86	1.86	1.9	1.91
Power Plant	2.77	27.33	2.95	2.95	0.91	0.51
Refinery	2.53	27.09	2.71	2.71	0.66	0.82

After acquiring the information of sources and sinks, the density of delivered fluid for each source-sink connection is calculated using PR EOS and mixing rules and critical properties from Aspen Plus in Table 8, and the result of the density for each connection presented in Table 9.

Table 8 Physical Properties of Mixture of Carbon Dioxide and Nitrogen at Critical Point

CO_2 Composition (wt%)	Pc (kPa)	Tc (K)	Vc (m^3/mol)	Zc	Cv (J/kmol-K)	Cp (J/kmol-K)	γ (Cp/Cv)
7 for Power Plant	3582.1	134.339	0.089	0.288	21227.3	29593.1	1.394
27 for Refinery	4159.02	160.122	0.090	0.286	22513	30893.4	1.372
44 for Steel Plant	4727.9	185.547	0.098	0.284	23782.6	32177.6	1.353

Table 9 Density of Fluid Mixture for each Source and Sink

Sink / Source	Algae / Greenhouse (101 kPa)	Methanol (8080 kPa)	Urea (14140 kPa)	EOR / Saline Storage (15198 kPa)
Ammonia Plant (100 wt%, 101 kPa)	1.713 kg/m^3 at 101 kPa, 469 kg/m^3 at 7376 kPa			
Steel Plant (44 wt%, 101 kPa)	1.296 kg/m^3 at 101 kPa, 381 kg/m^3 at 4728 kPa			
Refinery (27 wt%, 101 kPa)	1.209 kg/m^3 at 101 kPa, 355 kg/m^3 at 4159 kPa			
Power Plant (7 wt%, 101 kPa)	1.117 kg/m^3 at 101 kPa, 323 kg/m^3 at 3582.1 kPa			

For step 2 to calculate the pressure drop and the cost of every pipeline for each source-sink connection, the information of the nominal pipe size, outer diameter and inner diameter for each pipe the ASME / ANSI B.36 [54] and each internal cross-sectional area is presented in Table 10.

Table 10 Commercial Carbon Steel XS Grade Pipe Data ASME / ANSI B.36 [54]

Nominal Pipe Size (NPS, in)	Outer Diameter (OD, m)	Thickness (m)	Internal Diameter (ID, m)	Internal Area (A_p, m^2)
0.125	0.0103	0.00241	0.00548	0.0000359
0.250	0.0137	0.00302	0.00766	0.00004608
0.375	0.0171	0.0032	0.0107	0.00008992
0.5	0.02134	0.00373	0.01388	0.0001513
0.75	0.02667	0.00391	0.01885	0.0002791
1	0.0334	0.00455	0.0243	0.0004638
1.25	0.04216	0.00485	0.03246	0.0008275
1.5	0.04826	0.00508	0.0381	0.001140
2.0	0.06032	0.00554	0.04924	0.001904
2.5	0.07302	0.00701	0.059	0.002734
3	0.0889	0.00762	0.07366	0.004261
3.5	0.1016	0.00808	0.08544	0.005733
4	0.1143	0.00856	0.09718	0.007417
5	0.1413	0.00952	0.12226	0.01174
6	0.1683	0.01097	0.14636	0.01682
8	0.2191	0.0127	0.1937	0.02947
10	0.273	0.0127	0.2476	0.04815
12	0.3239	0.0127	0.2985	0.06998
14	0.3556	0.0127	0.3302	0.08563
16	0.4064	0.0127	0.381	0.114
18	0.4572	0.0127	0.4318	0.1464
20	0.508	0.0127	0.4826	0.1829
22	0.5588	0.0127	0.5334	0.2235
24	0.6096	0.0127	0.5842	0.2680
26	0.6604	0.0127	0.635	0.3167
28	0.7112	0.0127	0.6858	0.3694
30	0.762	0.0127	0.7366	0.4261
32	0.8128	0.0127	0.7874	0.4869
34	0.8636	0.0127	0.8382	0.5518
36	0.9144	0.0127	0.889	0.6207
40	1.016	0.0127	0.9906	0.7707
42	1.067	0.0127	1.0416	0.8521
44	1.118	0.0127	1.0926	0.9376
46	1.168	0.0127	1.1426	1.025
48	1.219	0.0127	1.1936	1.119
52	1.321	0.0127	1.2956	1.318
56	1.422	0.0127	1.3966	1.532

For step 3, since the adiabatic compression is assumed for this work, the increase of temperature in one stage is calculated using the relation of T_2/T_1 = (Compression Ratio) $^{(k-1)/k}$ where the value of k is set as 1.28 [62] considered as ideal one. Then, using the Properties Analysis in Aspen Plus with Peng-Robinson method, the information at the inlet pressure and outlet pressure for each compression stage is collected. Then the value of each property at inlet and outlet pressure is averaged out to apply the value to equation (36). Collected thermodynamic information is shown in Table 11.

Since over 6.0 of compression ratio is not recommended due to the safety concern [63], two stages of compression with 8.546 of compression ratio and 1 stage of compression with 73.03 of compression ratio are excluded in the compression optimization work.

Table 11 Thermodynamic Properties Data for Multi-Stage Compression

Compression Ratio (CR_h)	Compression Stage (h)	Inlet Pressure (P_{in}, kPa)	Outlet Pressure (P_{out}, kPa)	Average Z	Average k	Average ρ (kg/m^3)
1.5359	1	101	155	0.995	1.279	2.084
	2	155	238	0.992	1.282	3.211
	3	238	366	0.988	1.287	4.955
	4	366	562	0.981	1.296	7.664
	5	562	863	0.971	1.308	11.901
	6	863	1326	0.956	1.329	18.606
	7	1326	2036	0.931	1.366	29.399
	8	2036	3128	0.893	1.434	47.305
	9	3128	4804	0.831	1.578	78.776
	10	4804	7376	0.728	1.992	141.714
1.6109	1	101	162	0.995	1.279	2.120
	2	162	262	0.992	1.283	3.427
	3	262	422	0.986	1.289	5.551
	4	422	680	0.978	1.300	9.023
	5	680	1096	0.964	1.318	14.752
	6	1096	1765	0.942	1.350	24.359
	7	1765	2843	0.905	1.411	40.939
	8	2843	4580	0.843	1.549	71.177
	9	4580	7376	0.734	1.975	133.609
1.7098	1	101	173	0.995	1.279	2.174
	2	173	295	0.991	1.284	3.733
	3	295	505	0.984	1.292	6.426
	4	505	863	0.972	1.307	11.120
	5	863	1476	0.953	1.334	19.418
	6	1476	2523	0.918	1.389	34.489
	7	2523	4315	0.856	1.518	63.366
	8	4315	7376	0.740	1.958	125.970
1.846	1	101	186	0.995	1.275	2.244
	2	186	344	0.990	1.280	4.162
	3	344	635	0.982	1.290	7.752
	4	635	1173	0.967	1.310	14.554
	5	1173	2165	0.938	1.352	27.759
	6	2165	3997	0.884	1.452	54.722
	7	3997	7376	0.779	1.778	116.780
2.0445	1	101	206	0.995	1.272	2.352
	2	206	422	0.989	1.279	4.838
	3	422	863	0.978	1.293	10.018
	4	863	1765	0.955	1.324	21.039
	5	1765	3608	0.908	1.405	45.616
	6	3608	7376	0.807	1.678	107.328
2.3589	1	101	238	0.995	1.268	2.509
	2	238	562	0.988	1.276	5.967
	3	562	1326	0.972	1.298	14.354
	4	1326	3127	0.933	1.358	35.549
	5	3127	7376	0.840	1.578	95.412
2.9234	1	101	295	0.995	1.262	2.799
	2	295	863	0.985	1.275	8.285
	3	863	2523	0.957	1.316	25.130
	4	2523	7376	0.875	1.487	82.474
4.18	1	101	422	0.995	1.254	3.426
	2	422	1765	0.979	1.277	14.645
	3	1765	7376	0.916	1.396	67.240

Since the allowable flow range for each source-sink connection was set by considering the maximum capacity of each source and sink, and the flow range is divided into 19 intervals to make 20 segments of flow rates. The minimum total annualized costs for the 20 flow rates are calculated and plotted. Then, the linear cost model for each source-sink connection was established and presented in Table 12.

Table 12 Linear Transportation Cost Models of Untreated Flow

Source	Sink	Flow Range (MTPD)	Cost Model $c_{s,k}U_{s,k} + d_{s,k}$ (USD/yr)	R^2	Flow Range (MTPD)	Cost Model $c_{s,k}U_{s,k} + d_{s,k}$ (USD/yr)	R^2
Ammonia Plant	Algae	10~200	960.88Us,k+ 66305	0.923	~300	564.39Us,k+ 96932	0.945
	Greenhouse	10~264.5	10811Us,k+ 1122118	1	~977	3788Us,k+ 2872287	1
	Storage	10~977	874.43Us,k+ 51621	0.999	-	-	-
	Methanol	10~977	802.61Us,k+ 51621	0.999	-	-	-
	Urea	10~977	864.79Us,k+ 52327	0.999	-	-	-
	EOR	10~977	875.73Us,k+ 52503	0.999	-	-	-
Steel Plant	Algae	10~2000	362Us,k+ 265565	1	~4400	141Us,k+ 457535	1
	Greenhouse	10~2000	3732Us,k+ 2392802	1	~4400	1746Us,k+ 5629596	1
	Storage	10~4500	875.61Us,k+ 97391	0.999	-	-	-
	Methanol	10~1710	815.22Us,k+ 72073	0.999	-	-	-
	Urea	10~1130	920.77Us,k+ 62634	0.999	-	-	-
	EOR	10~2740	887.09Us,k+ 88822	0.999	-	-	-
Power Plant	Algae	10~1800	459Us,k+ 236828	1	~4400	183Us,k+ 672943	1
	Greenhouse	10~1800	4511Us,k+ 2308575	1	~4400	1795Us,k+ 6604730	1
	Storage	10~6800	557.65Us,k+ 117079	0.999	-	-	-
	Methanol	10~1710	822.73Us,k+ 95026	0.998	-	-	-
	Urea	10~1126	885.3Us,k+ 43370	0.999	-	-	-
	EOR	10~2736	855.89Us,k+ 54388	0.999	-	-	-
Refinery	Algae	10~2000	369Us,k+ 237497	1	~4400	172Us,k+ 558850	1
	Greenhouse	10~2000	3928Us,k+ 2518707	1	~4400	1838Us,k+ 5925439	1
	Storage	10~1092	957.57Us,k+ 77975	0.998	-	-	-
	Methanol	10~1092	862.72Us,k+ 77975	0.998	-	-	-
	Urea	10~1092	889.88Us,k+ 38722	0.999	-	-	-
	EOR	10~1092	908.16Us,k+ 41785	0.999	-	-	-

Table 13 Linear Transportation Cost Models of Treated Flow

Source	Sink	Flow Range (MTPD)	Cost Model $e_{s,k,t}\,T_{s,k,t} + f_{s,k,t}$ (USD/yr)	R^2	Flow Range (MTPD)	Cost Model $e_{s,k,t}\,T_{s,k,t} + f_{s,k,t}$ (USD/yr)	R^2
Ammonia Plant	Algae	10~200	960.88 $T_{s,k,t}$ + 66305	0.923	~300	564.39 $T_{s,k,t}$ + 96932	0.945
	Greenhouse	10~264.5	10811 $T_{s,k,t}$ + 1122118	1	~977	3788 $T_{s,k,t}$ + 2872287	1
	Storage	10~977	874.43 $T_{s,k,t}$ + 51621	0.999	-	-	-
	Methanol	10~977	802.61 $T_{s,k,t}$ + 51621	0.999	-	-	-
	Urea	10~977	864.79 $T_{s,k,t}$ + 52327	0.999	-	-	-
	EOR	10~977	875.73 $T_{s,k,t}$ + 52503	0.999	-	-	-
Steel Plant	Algae	10~100	1324 $T_{s,k,t}$ + 74971	1	~285	680 $T_{s,k,t}$ + 124730	1
	Greenhouse	10~278	10401 $T_{s,k,t}$ + 1143491	1	~1030	3680 $T_{s,k,t}$ + 3017894	1
	Storage	10~3451	816.92 $T_{s,k,t}$ + 95665	0.999	-	-	-
	Methanol	10~1710	779 $T_{s,k,t}$ + 70394	0.999	-	-	-
	Urea	10~1130	864.95 $T_{s,k,t}$ + 61015	0.999	-	-	-
	EOR	10~2740	828.2 $T_{s,k,t}$ + 87125	0.999	-	-	-
Power Plant	Algae	10~115	1631.7 $T_{s,k,t}$ + 105797	0.922	~285	956.87 $T_{s,k,t}$ + 156481	0.945
	Greenhouse	10~278	11050 $T_{s,k,t}$ + 1214409	1	~1030	3910 $T_{s,k,t}$ + 3205093	1
	Storage	10~4400	800.53 $T_{s,k,t}$ + 167247	0.999	-	-	-
	Methanol	10~1710	800.03 $T_{s,k,t}$ + 92193	0.998	-	-	-
	Urea	10~1126	841.26 $T_{s,k,t}$ + 43097	0.999	-	-	-
	EOR	10~2736	806.91 $T_{s,k,t}$ + 55309	0.999	-	-	-
Refinery	Algae	10~100	1632 $T_{s,k,t}$ + 91454	1	~283	838 $T_{s,k,t}$ + 152283	1
	Greenhouse	10~280	10952 $T_{s,k,t}$ + 1203778	1	~1030	3875 $T_{s,k,t}$ + 3177020	1
	Storage	10~1092	897.6 $T_{s,k,t}$ + 74611	0.998	-	-	-
	Methanol	10~1092	825.78 $T_{s,k,t}$ + 74611	0.998	-	-	-
	Urea	10~1092	836.62 $T_{s,k,t}$ + 38079	0.999	-	-	-
	EOR	10~1092	851.23 $T_{s,k,t}$ + 40931	0.999	-	-	-

6.3 Results of the Optimizing CO_2 Transportation Cost

Developed linear cost models in Table 12 and Table 13 substituted the cost of transportation part of the source-sink matching result from Al-Mohannadi and Linke [51] to confirm the cost-saving from this work. Then linear cost models are applied to the MINLP formulations of Al-Mohannadi and Linke [51] to change them into MILP problem with modified objective functions in Table 3 for the global optimization of carbon

integration network under six carbon reduction target: 3%, 10%, 20%, 30%, 40% and 50%.

Firstly, based on connections and flow rates of previous work, the new transport design suggested in this work is applied to calculate the total annualized transportation cost as the control group. Then the transportation-optimizing design is applied to the new transport design, and it presented cost-savings from 7 to 9 percent of total annualized transportation cost. The cost-savings from the compression appeared in every carbon reduction target, and showed gradual savings by optimizing the compression stages to decrease the power consumption for the compression. Due to the small portion of the transport cost compared to the treatment cost, the effect of transportation-optimizing design displayed little cost-saving in total carbon integration network cost. Based on same condition, the linear transportation cost models is applied to calculate the total transportation cost and it showed high accuracy with 0.03%~0.8% difference. The result of the transportation-optimizing design is presented in Table 14 and Figure 10.

Table 14 Results Comparison of Total Annualized Transportation Cost

		Pure CO_2 Stream			Impure Stream			TAC, total (USD/yr)	Cost Savings
		AC, pipe	AC, comp	TAC, pure	AC, pipe	AC, comp	TAC, impure		
3%	New Transport Design	41691	628906	670597	0	0	0	670597	53964
	Transport-optimized Design	48599	568028	616627	0	0	0	**616627**	
10%	New Transport Design	154199	2397911	2552110	0	0	0	2552110	209883
	Transport-optimized Design	140383	2201844	2342227	0	0	0	**2342227**	
20%	New Transport Design	256545	4062738	4319283	695004	11926	706930	5026212	421840
	Transport-optimized Design	231747	3706134	3937881	650187	16304	666491	**4604372**	
30%	New Transport Design	295954	6244356	6540310	1398767	27656	1426423	7966733	540533
	Transport-optimized Design	280566	5719212	5999777	1398767	27656	1426423	**7426200**	
40%	New Transport Design	437207	8419916	8857124	1398767	27656	1426423	10283546	789442
	Transport-optimized Design	411657	7656024	8067681	1398767	27656	1426423	**9494104**	
50%	New Transport Design	525899	10480876	11006775	1398767	27656	1426423	12433198	969433
	Transport-optimized Design	488569	9548773	10037342	1398767	27656	1426423	**11463765**	

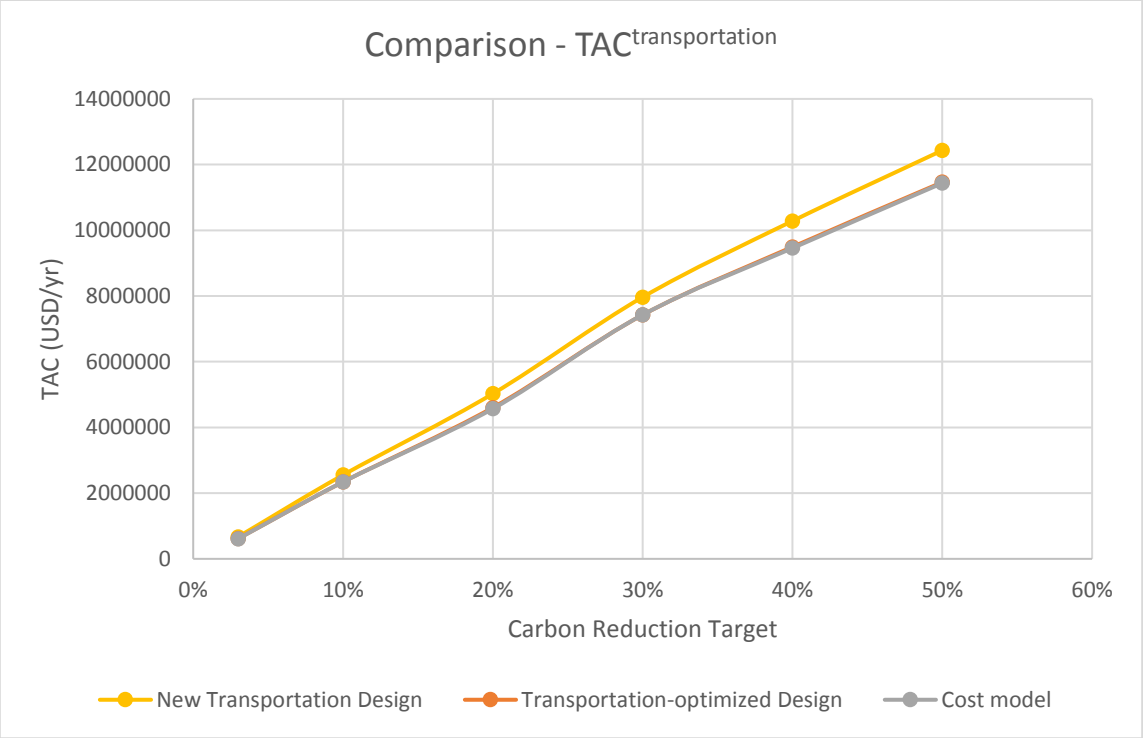

Figure 10 Comparison of Total Annualized Transportation Cost

Then, developed linear cost models are implemented to the global optimization work of the carbon integration network. For the global optimization work, "What's Best 9.0" Lindo Global [64] solver for MS Excel® 2013 was used via a laptop with Intel Core® i7 processor, 8GB RAM and a 64-bit Windows® system.

In 3% reduction target, original work result from Al-Mohannadi and Linke [51] and the transportation-optimizing work showed same carbon allocation which is from the ammonia plant to the EOR site based on the sink-load rule in 3% reduction target. Both cases show 614 ton of net CO_2 captured. And the total cost for the transportation-optimizing work is USD -6.33 million per year while the original model shows USD -6.32

million per year. Thus, modified work shows USD -28.25 per ton of CO_2 captured while the original work showed USD -28.21 per ton of CO_2 captured.

For the 10% of target, 2046 ton of CO_2 is captured. The total cost of the transportation-optimizing work shows USD -10.1 million per year and the original one is USD -10.4 million per year; thus, the cost of capture per ton of CO_2 for the optimization work is USD -13.49 per ton of CO_2 while USD -13.87 per ton CO_2 costs for the original model. This is because more revenue is produced from the original work than the optimization work.

Under the 20% of target with 4092.8 ton of net CO_2 captured, the total cost of the transportation-optimizing work shows USD -2.56 million per year while the original result only achieves USD -1.93 million per year while the connections are similar each other. Thus, capture cost per ton of CO_2 for the modified model presents USD -1.72 per ton of CO_2 captured while original result only shows USD -1.29 per ton of CO2 captured. This case shows that the optimization work is successful when it has the same connection with the original work.

From 30% of the target, both the original and the transportation-optimizing work turned to the positive capture costs which means carbon integration network requires capital investment for high carbon reduction target. Each total carbon integration cost is USD 39.7 million per year for the optimization work and USD 43 million per year for the original one. And each capture cost per ton of CO_2 is USD 17.73 per ton of CO_2 for the modified model and USD 19.18 per ton of CO_2 for the original one.

For the 40% of target, each total cost per year is USD 81.9 million per year for the transportation-optimizing work and USD 86 million per year for the original work. Each capture cost per ton of CO2 is USD 27.42 per ton of CO_2 for the transportation-optimizing work and USD 28.78 per ton of CO2 for the original model. Both higher profit and cheaper transportation cost dedicated to cost-savings in this case.

The 50% of target is very crucial to implement the CCUS system while some countries pledged to reduce their emission more than 45% [65]. Under 50% of reducing target, each total annual cost is USD 125 million per year for the transportation-optimizing work and USD 126 million per year for the original work. And each capture cost per ton of CO_2 is USD 33.49 per ton of CO_2 for the optimization work and USD 33.75 per ton of CO_2 for the original model.

The global optimization results of the carbon integration network showed improved economic, but it does not have huge impact on the total carbon integration cost. To confirm this, Figure 11 for the carbon integration cost per ton of CO_2 versus carbon reduction target and Figure 12 for cost components of carbon integration are plotted. As seen in these two figures, the portion of transportation is around 10% of treatment cost with little impact on the total carbon integration cost. Thus, developing the CCUS system with low treatment cost is required to overcome USD 25~30 per ton of CO_2 captured suggested as a carbon tax range in carbon-reduction leading countries [66], [67]

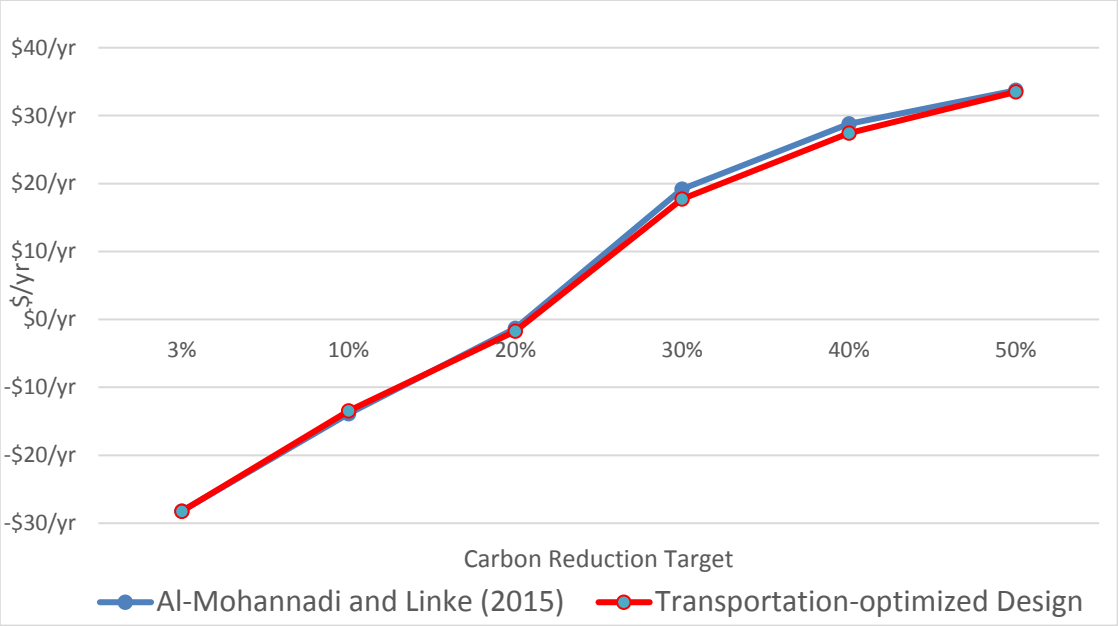

Figure 11 Comparison of Specific Carbon Integration Network Cost

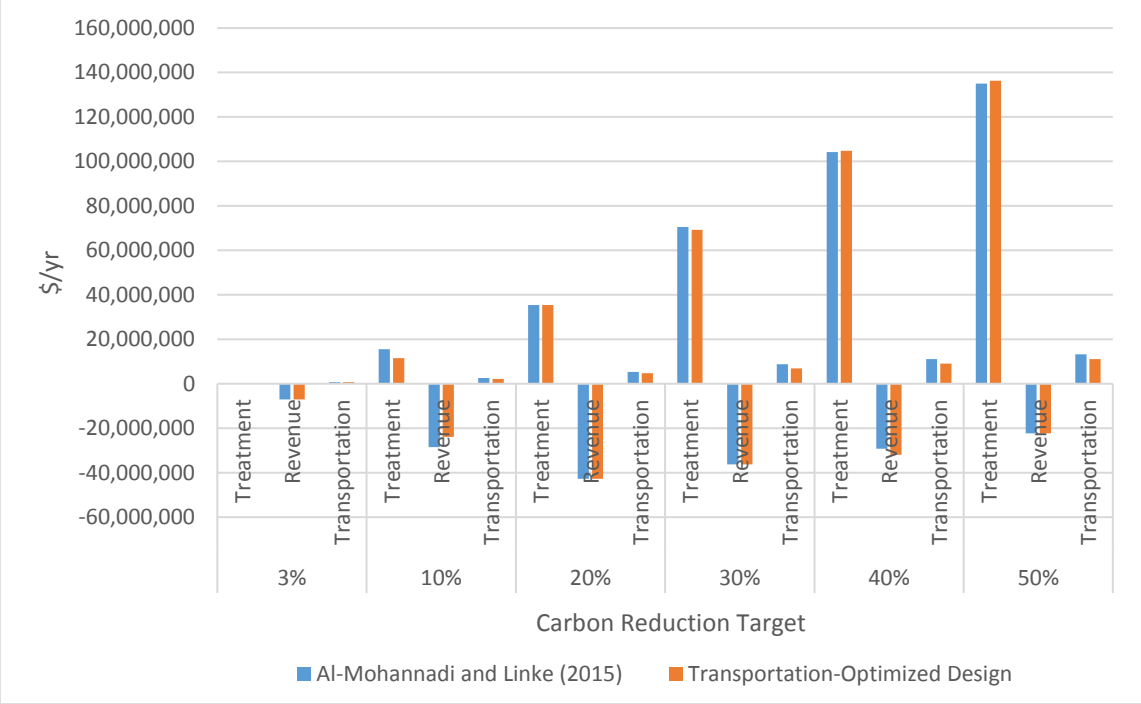

Figure 12 Comparison of Cost Components of Carbon Integration Network

7. COST MINIMIZATION OF CARBON TREATMENT

In this section, linear cost models of multiple carbon treatment technologies will be introduced by modifying the input-output based cost models of Hasan et al. [52], [53] based on the source and sink information from Al-Mohannadi and Linke [51], and the results are compared to confirm the improvements.

7.1 Prerequisites for the Establishment of Cost Models for the Treatment Process

Although numerous works have been conducted to build cost models of various treatment technologies, most of them considered fixed source composition and flow rate only. However, since this work deals with different CO_2 emission source, it is desired to find the well-documented models which consider the effect of composition and flow rate simultaneously. Hasan et al. [52], [53] introduced the cost models of amine absorption, gas separation membrane, pressurized swing adsorption and vacuum swing adsorption as functions of composition and flow rate which show 90% of recovery and purity as presented in Table 15. Therefore, this work will adopt the black-box cost model from Hasan et al. [52], [53] to construct cost models of multiple carbon treatment technologies for each source.

Table 15 Cost Models of Hasan et al. [52], [53]

$\alpha + (\beta x_{co2}^{n} + \gamma) F^{m}$	Process	α	β	γ	n	m	x_{co2} (mol%)	F (mol/s)
Investment Cost (USD/yr)	Absorption	7719	67871	901	0.66	0.80	0.01 $<x_{co2}<$ 0.70	100 < F < 10000
	Membrane	177500	16505	18192	0.88	0.77		
	PSA	206010	9601	5731	1	0.832		
	VSA	168128	11531	4793	1	0.82		
Operating Cost (USD/yr)	Absorption	0	24088	0	1	1		
	Membrane	0	11619	0	0.21	1		
	PSA	0	4954	7406	0.93	1		
	VSA	0	3992	5857	0.743	1		

However, these cost models are based on different economic and other assumptions from Al-Mohannadi and Linke [51], and should be linearized to be applied for the formulations of MILP; thus, applying same economic assumption with Al-Mohannadi and Linke [51] and linearization work is conducted for establishing suitable cost models to convert MINLP into MILP problem.

Firstly, the capital and operating cost for compression up to 150 bar were excluded from every treatment costs. To eliminate the cost of compression from Hasan et al. [52], [53], the capital and operating cost for the compression based on the work of compression computed using below equations were deducted from the total annualized treatment costs.

$$W^{comp\prime} = \frac{6 \times 0.9 \times m}{0.75} \times \left(\frac{8314}{745.3}\right) \times 308 \times \frac{1.4}{1.4-1} \times (2.3^{(\frac{1.4-1}{1.4})} - 1) \quad (44)$$

$$CC^{cap\prime} = 0.154 \times 3791.3 \times \left(\frac{109}{103}\right) \times \left(\frac{W^{comp\prime}}{0.7453}\right)^{0.82} \quad (45)$$

$$CC^{oper\prime} = 8000 * 0.07 \times W^{comp\prime} \quad (46)$$

where $W^{comp'}$: Work done by the compression in the model from Hasan et al. [52], [53], $CC^{cap'}$: Capital cost of the compression in the model from Hasan et al. [52], [53], $CC^{oper'}$: Operating cost of the compression in the model from Hasan et al. [52], [53].

Secondly, economic factors and assumptions were changed from Hasan et al. [52], [53] to Al-Mohannadi and Linke [60]. Capital recovery factor (CRF) is changed from 0.154 to 0.15, and the cost of electricity (COE) is changed from 0.07 USD / kWh to 0.02 USD / kWh. Additionally, 2552.2 for 2015 and 2465.2 for 2012 of Nelson-Farrar cost indexes [68] is applied to linearized cost models while Hasan et al. [52], [53] were published in 2012 and Al-Mohannadi and Linke [51] is published in 2015.

Hereafter, treatment technologies will be called as following abbreviation: amine absorption as ABS, gas separation membrane as MEMB and vacuum swing adsorption as VSA.

7.2 Establishments of Cost Models of the Treatment Process

Since the cost models from Hasan et al. [52], [53] have two variables, molar composition and molar flow rate; it is desired to express them into the linear function of mass flow rate. Thus, cost models from Hasan et al. [52], [53] are expanded by flow rate range under specific composition sets, and total costs of multiple treatments versus mass

flow rate equivalent to molar flow rate are plotted. From these plots, linear cost models are derived which have $a_{s,t}$, $b_{s,t}$ as coefficients.

First, molar flow rates based on weight compositions of sources from Al-Mohannadi and Linke [51] were calculated while cost models from Hasan et al. [52], [53] are functions of molar composition and molar flow.

$$m = 3600 * 24 * (mol\% * M * 44 + (1 - mol\%) * M * 28)/(1000000) \quad (47)$$

where m: Molar flow rate (mol/s), M: Mass flow rate (MTPD), mol%: Mole fraction of CO2 from the source.

Then sets of molar flow rate based total annualized treatment costs for each treatment technology are calculated.

After achieving sets of total annualized treatment costs, the linearization works were conducted for amine absorption (ABS), gas separation membrane (MEMB) and vacuum swing adsorption (VSA) technologies considering every source composition except the ammonia plant since the ammonia plant produces only pure CO_2. While the linearization works, it was possible to estimate the economic priority of each technology for certain emission source graphically. According to the plots from Figure 13, Figure 14 and Figure 15, ABS for the power plant and VSA for both the steel plant and the refinery showed more economically priority than other technologies. Thus, in the later section, these technologies will be selected for the confirmation of economic effect. And PSA technologies are excluded while it has a less economic effect compared with VSA. The result of this work is presented in Table 16.

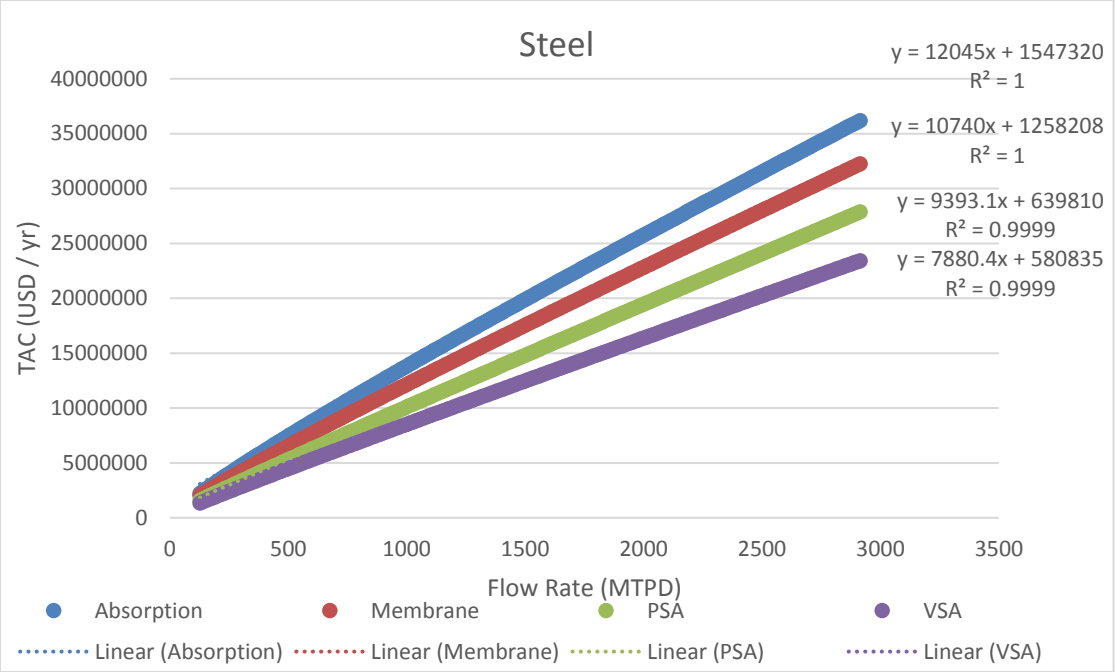

Figure 13 Optimized Treatment Linear Cost Models for the Steel Plant

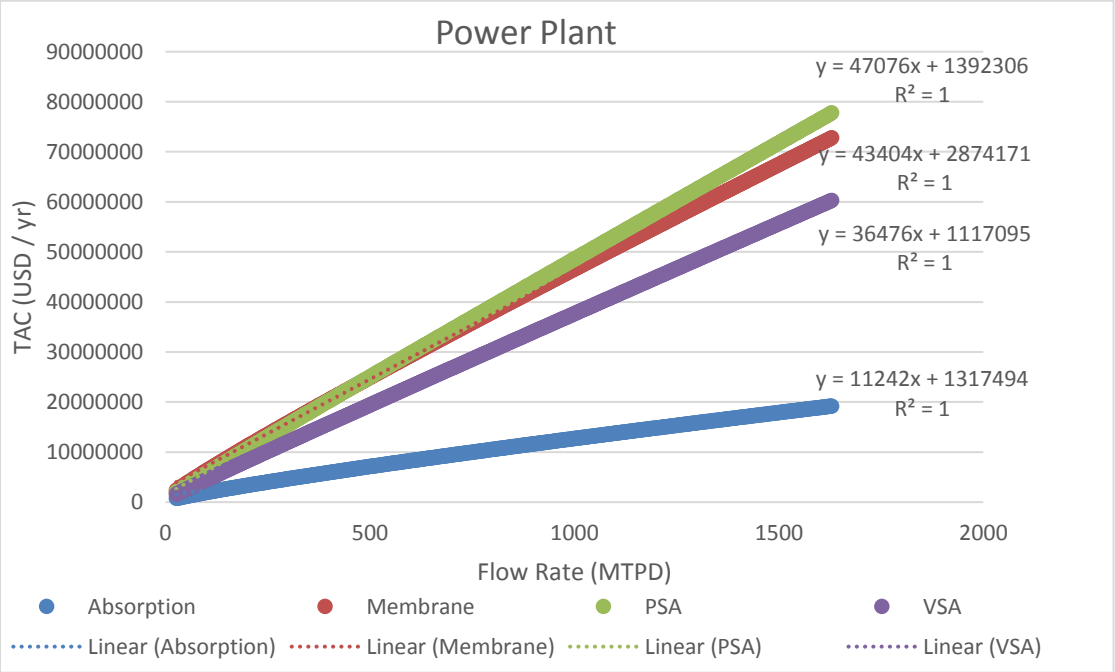

Figure 14 Optimized Linear Cost Models for the Power Plant

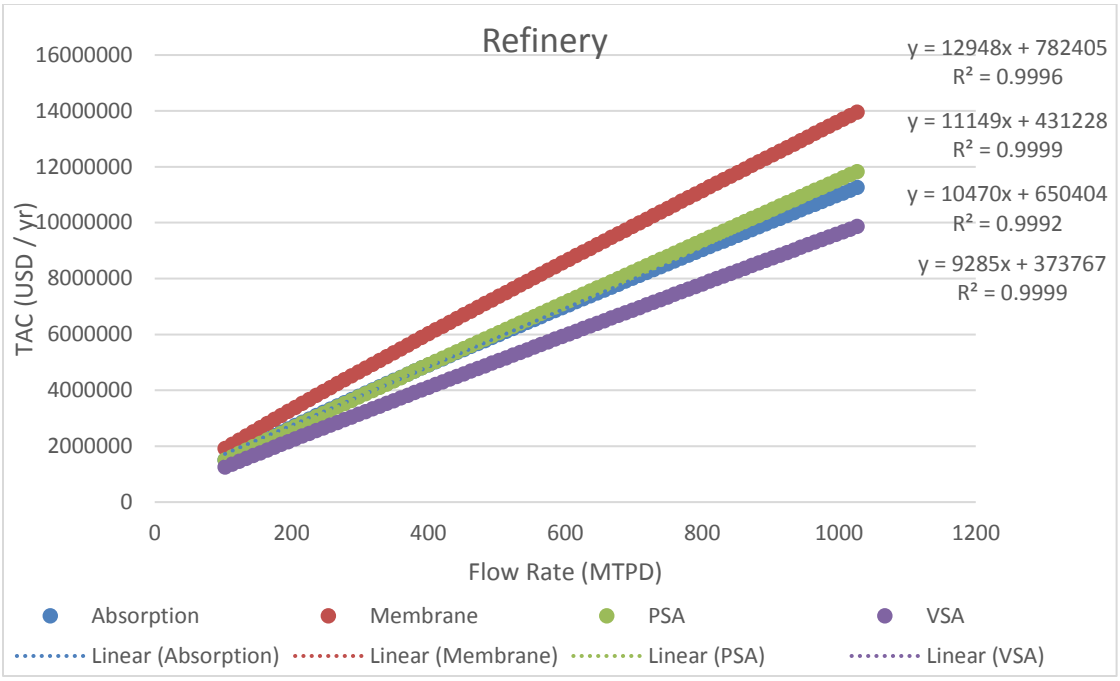

Figure 15 Optimized Linear Cost Models for the Refinery

Table 16 Cost Models of Each Treatment Technology for Each Carbon Emission Source

	Cost Models for Each Treatment Technology $C_{s,k,t}^{Treatment}$ (USD / yr)= $a_{s,t}(\sum X_{s,k}T_{s,t}) + b_{s,t}$								
	Chemical Absorption (ABS)			Membrane Gas Separation (MEMB)			Vacuum Swing Adsorption (VSA)		
Sources	Flow Range (MTPD)		R^2	Flow Range (MTPD)		R^2	Flow Range (MTPD)		R^2
	$a_{s,t}$	$b_{s,t}$		$a_{s,t}$	$b_{s,t}$		$a_{s,t}$	$b_{s,t}$	
Steel-Iron Plant	12045	1547320	1	10740	1258208	1	7880.4	580835	0.999
Power Plant	11242	1317494	1	43404	2874171	1	36476	1117095	1
Refinery	10470	650404	0.999	12498	782405	0.999	9285	373767	0.999

7.3 Results of the Optimizing CO_2 Treatment Cost

In spite of the effort to reduce the carbon integration cost by optimizing the transportation cost, it was not possible to achieve less overall costs than suggested carbon tax. However, in this section, it was possible to achieve the less overall expenditure than only considering the pipeline cost reduction by considering multiple types of treatment technologies and their cost models.

In this section, each carbon integration network case which meets each 3%, 10%, 20%, 30%, 40% and 50% of the carbon reduction target is investigated by applying new cost models of the treatment process. To evaluate the effect of changing each cost model of treatment technology, three cases of simulation were conducted: i) applying one treatment technology which showed the best economic performance for each source mentioned in section 6.3 (VSA for the steel plant and the refinery, ABS for the power plant), ii) applying two treatment technologies simultaneously (ABS-MEMB, ABS-VSA) and selecting only one competitive technology.

In the 3% of target, all three cases showed similar allocation results with the original work. This is because mainly pure CO_2 from the ammonia plant which does not require any treatment process was utilized only. The total carbon integration cost for every case is USD -7 million per year for case i), ii) with ABS-MEMB and ii) with ABS-VSA. Specific carbon integration cost for every case is USD-28.52 per ton of CO_2 net captured for case i), ii) with ABS-MEMB and ii) with ABS-VSA. For the carbon treatment cost per ton for each case is presented in Table 17. The allocation results are shown in Figure 16.

Table 17 Specific Cost of Each Treatment Option in 3% Target

3% target (USD / tCO_2)	Source / Option	Steel-Iron Plant	Power Plant	Refinery
Transportation-optimizing design	ABS	29	43.15	34.8
Case i)	ABS	-	-	-
	VSA	-	-	-
Case ii) -1	ABS	-	-	-
	MEMB	-	-	-
Case ii) -2	ABS	-	-	-
	VSA	-	-	-

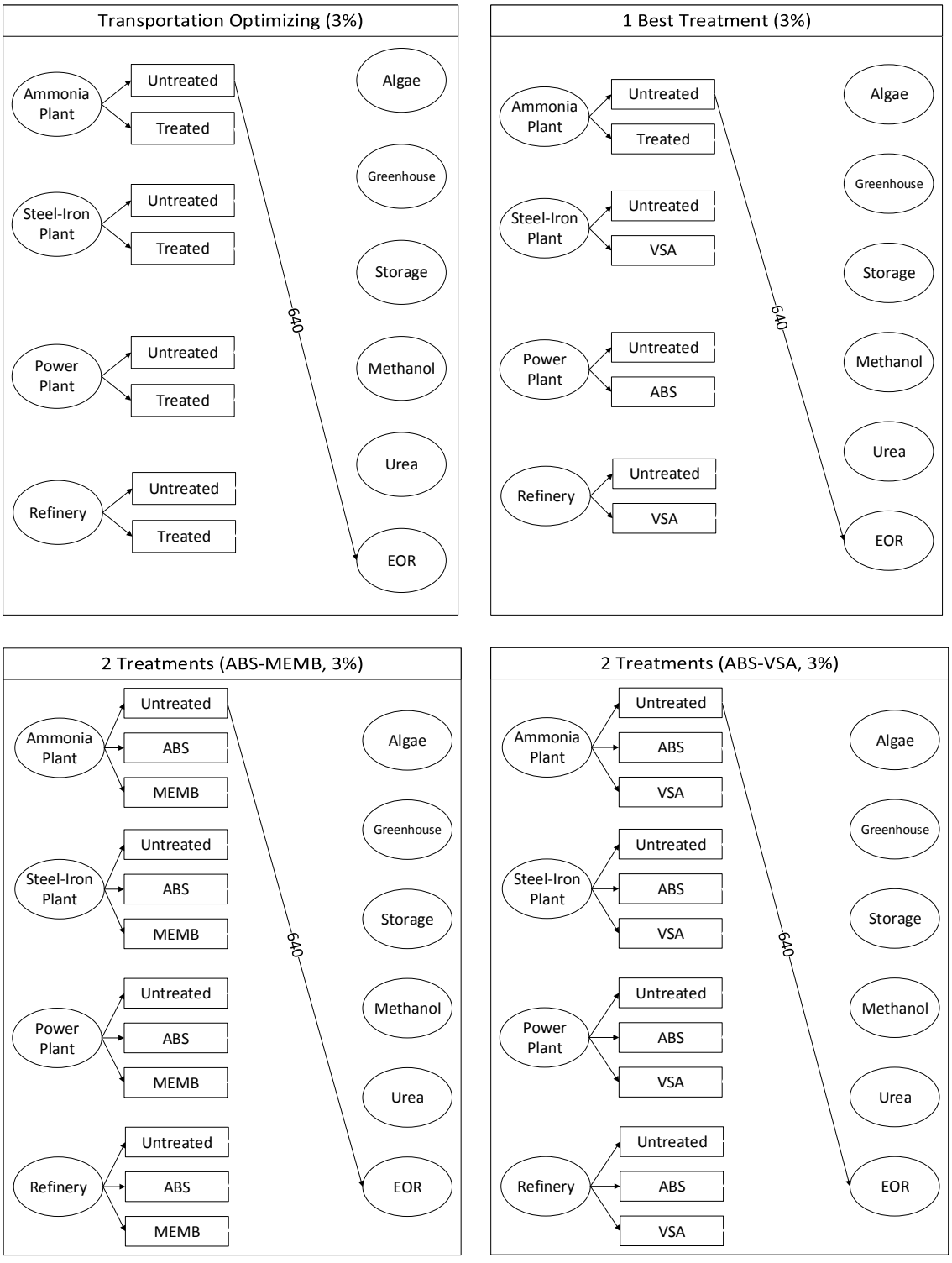

Figure 16 Carbon Allocations with Multiple Treatment Technologies for 3% Target

Under the 10% of reduction target, the total cost for each case is USD -13.8 million per year for case i) and ii) with ABS-VSA, and case ii) with ABS-MEMB showed USD -9.7 million per year. Capture cost for each case is USD -18.54 per ton of CO_2 net captured for all cases except case ii) with ABS-MEMB, USD -12.98 per ton of CO_2 net captured for case ii) with ABS-MEMB. In spite of same allocations, case ii) with ABS-MEMB showed higher treatment cost, because VSA is not available in this case and ABS is chosen as an alternative treatment technology always. In addition, the each case generated cheaper result than the result of Section 6. The allocation results are shown in Figure 17. The specific treatment costs were presented in Table 18.

Table 18 Specific Cost of Each Treatment Option in 10% Target

10% target (USD / tCO_2)	Source / Option	Steel-Iron Plant	Power Plant	Refinery
Transportation-optimizing design	ABS	29	43	35
Case i)	ABS	-	-	-
	VSA	-	-	-
Case ii) -1	ABS	-	-	-
	MEMB	32	-	-
Case ii) -2	ABS	-	-	-
	VSA	23	-	-

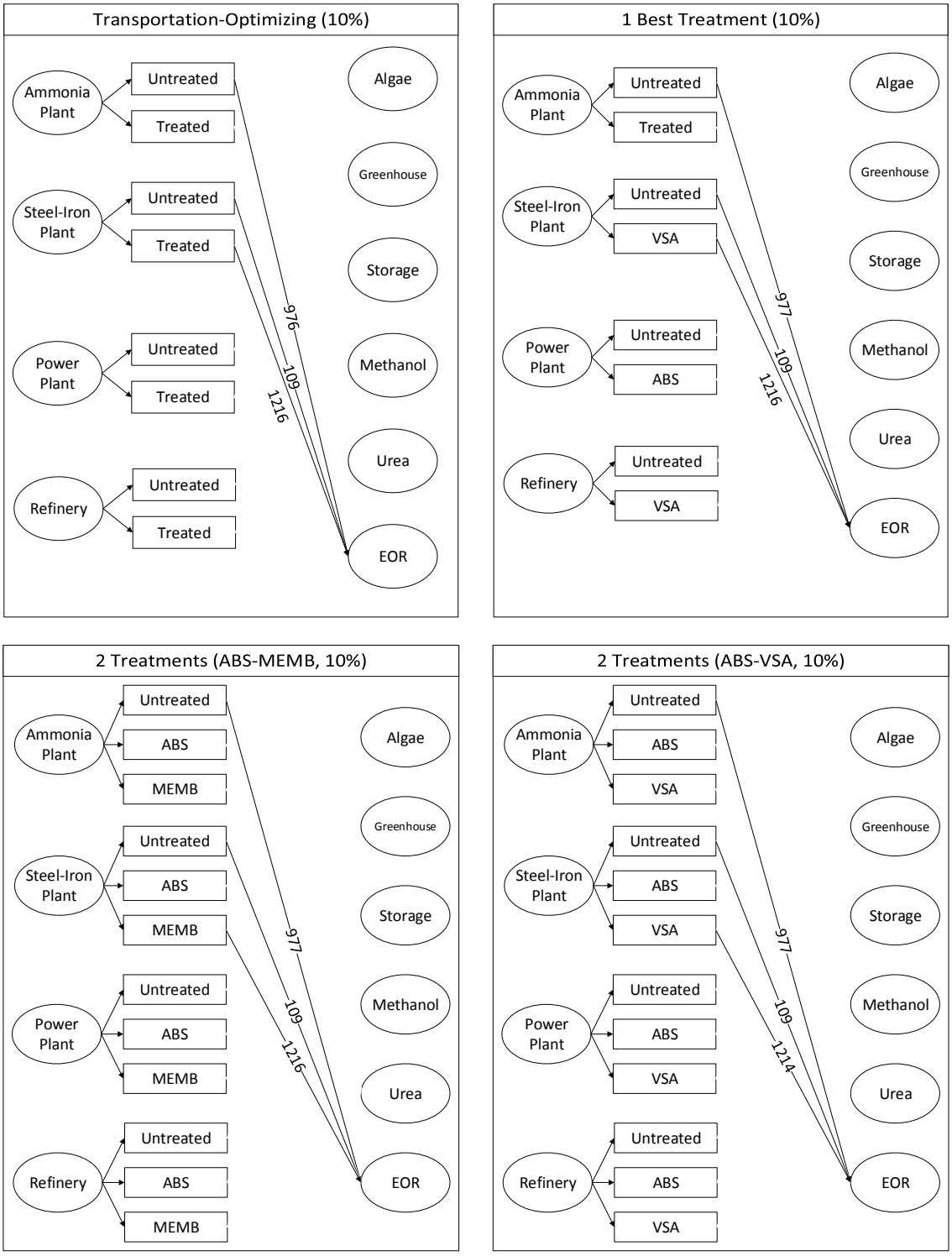

Figure 17 Carbon Allocations with Multiple Treatment Technologies for 10% Target

When the target is increased to 20%, the total cost for every case except ii) with ABS-MEMB is USD -14.7 million per year. And USD –3.8 million per year for case ii) with ABS-MEMB is presented. The specific carbon integration cost for every case except ii) with ABS-MEMB is USD -9.9 per ton of CO_2 net captured. USD -2.56 per ton of CO_2 net captured is for case ii) with ABS-MEMB. In case ii) with ABS-MEMB, the treatment cost decreased due to the scale of economic while ABS is only selected as the treatment option. The allocation results are displayed in Figure 18, and the specific treatment costs were presented in Table 19.

Table 19 Specific Cost of Each Treatment Option in 20% Target

20% target (USD / tCO_2)	Source / Option	Steel-Iron Plant	Power Plant	Refinery
Transportation-optimizing design	ABS	29	43	35
Case i)	ABS	-	-	-
	VSA	22	-	29
Case ii) -1	ABS	-	-	-
	MEMB	-	30	-
Case ii) -2	ABS	-	-	-
	VSA	22	-	29

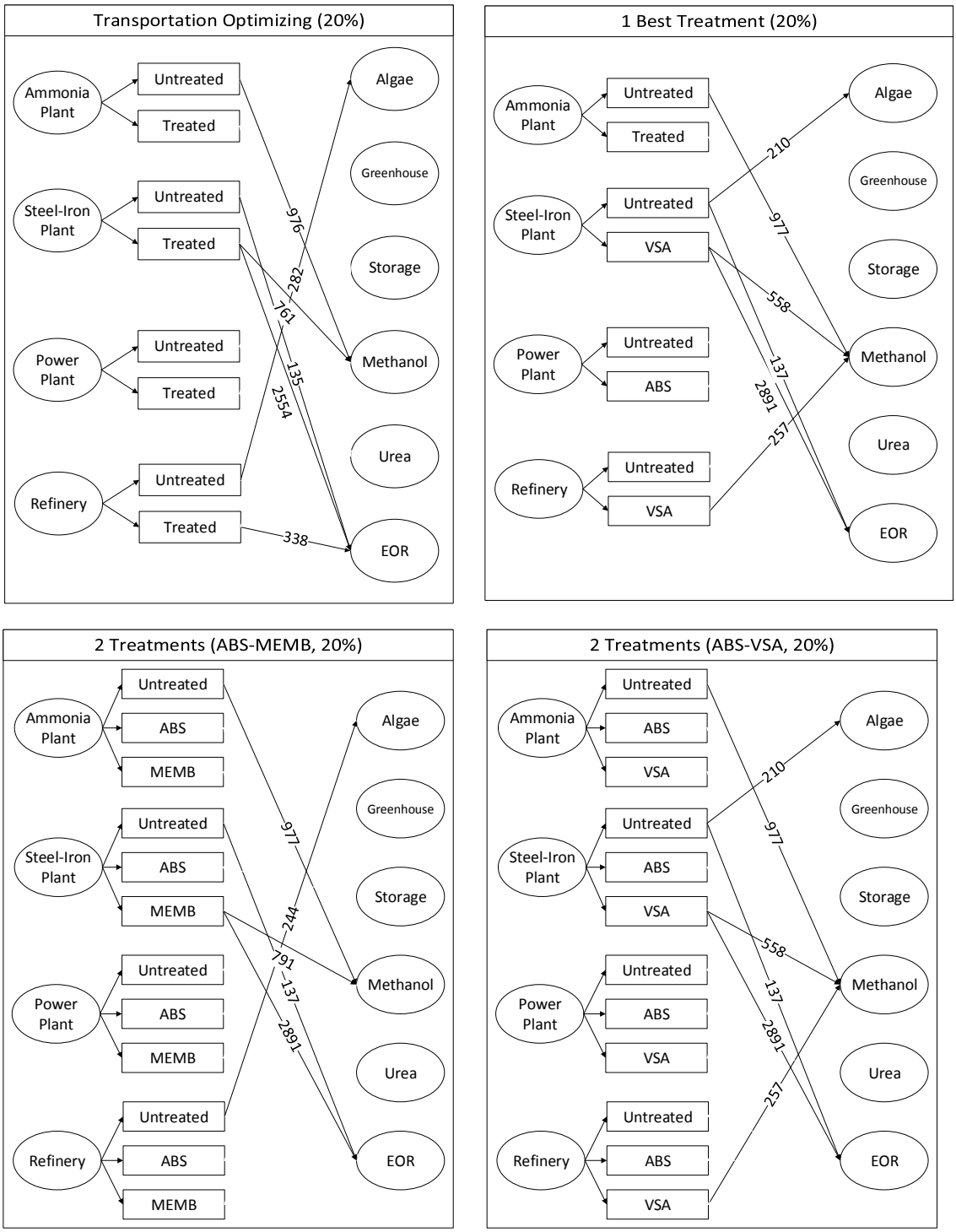

Figure 18 Carbon Allocations with Multiple Treatment Technologies for 20% Target

When the target is set to 30%, the total cost for each case is USD 16.8 million per year for case i), USD 36.5 million per year for case ii) with ABS-MEMB, and USD 22.5 million per year for case ii) with ABS-VSA. Capture cost for each case is USD 7.50 per ton of CO_2 net captured for case i), USD 10.04 per ton of CO_2 net captured for case ii) with ABS-VSA, and USD 16.27 per ton of CO_2 net captured for case ii) with ABS-MEMB. From 30% target, all the sources are involved in the CCUS system, and total expenditure exceeds the total revenue for every case. This is because the power plant which requires the most expensive treatment cost due to the most dilute CO_2 composition is included in the system. Also, it is possible to confirm that the cheapest treatment option is selected for each source as presented in Figure 19 and Table 20.

Table 20 Specific Cost of Each Treatment Option in 30% Target

30% target (USD / tCO_2)	Source / Option	Steel-Iron Plant	Power Plant	Refinery
Transportation-optimizing design	ABS	29	43	35
Case i)	ABS	-	33	-
	VSA	-	-	-
Case ii) -1	ABS	-	31	34
	MEMB	-	-	-
Case ii) -2	ABS	-	32	-
	VSA	22	-	26

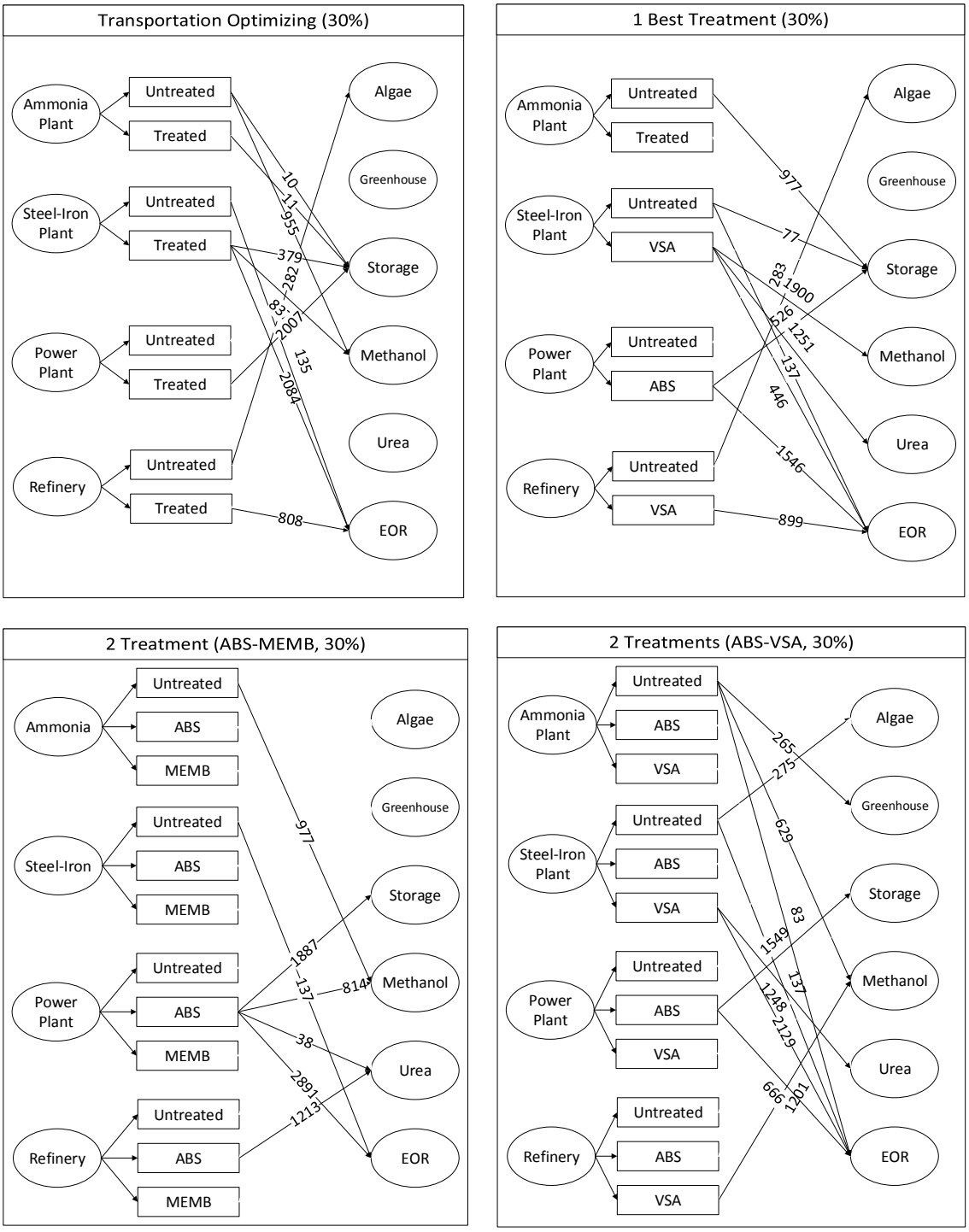

Figure 19 Carbon Allocations with Multiple Treatment Technologies for 30% Target

In the scenario of 40% of target, the total cost for each case is USD 53 million per year for case i) and ii) with ABS-VSA, and USD 77 million per year for case ii) with ABS-MEMB. Capture cost for each case is USD 17.72 per ton of CO_2 net captured for case i) and ii) with ABS-VSA, USD 25.76 per ton of CO_2 net captured for case ii) with ABS-MEMB. In case ii) with ABS-MEMB, although the membrane technology showed cheaper treatment cost model than the model of the amine absorption technology, global optimization work selected the amine absorption technology only due to the scale of the economy. The allocation result for 40% is shown in Figure 20, and the specific treatment cost is presented in Table 21.

Table 21 Specific Cost of Each Treatment Option in 40% Target

40% target (USD / tCO_2)	Source / Option	Steel-Iron Plant	Power Plant	Refinery
Transportation-optimizing design	ABS	29	43	35
Case i)	ABS	-	32	-
	VSA	22	-	27
Case ii) -1	ABS	38	32	34
	MEMB	-	-	-
Case ii) -2	ABS	-	32	-
	VSA	22	-	27

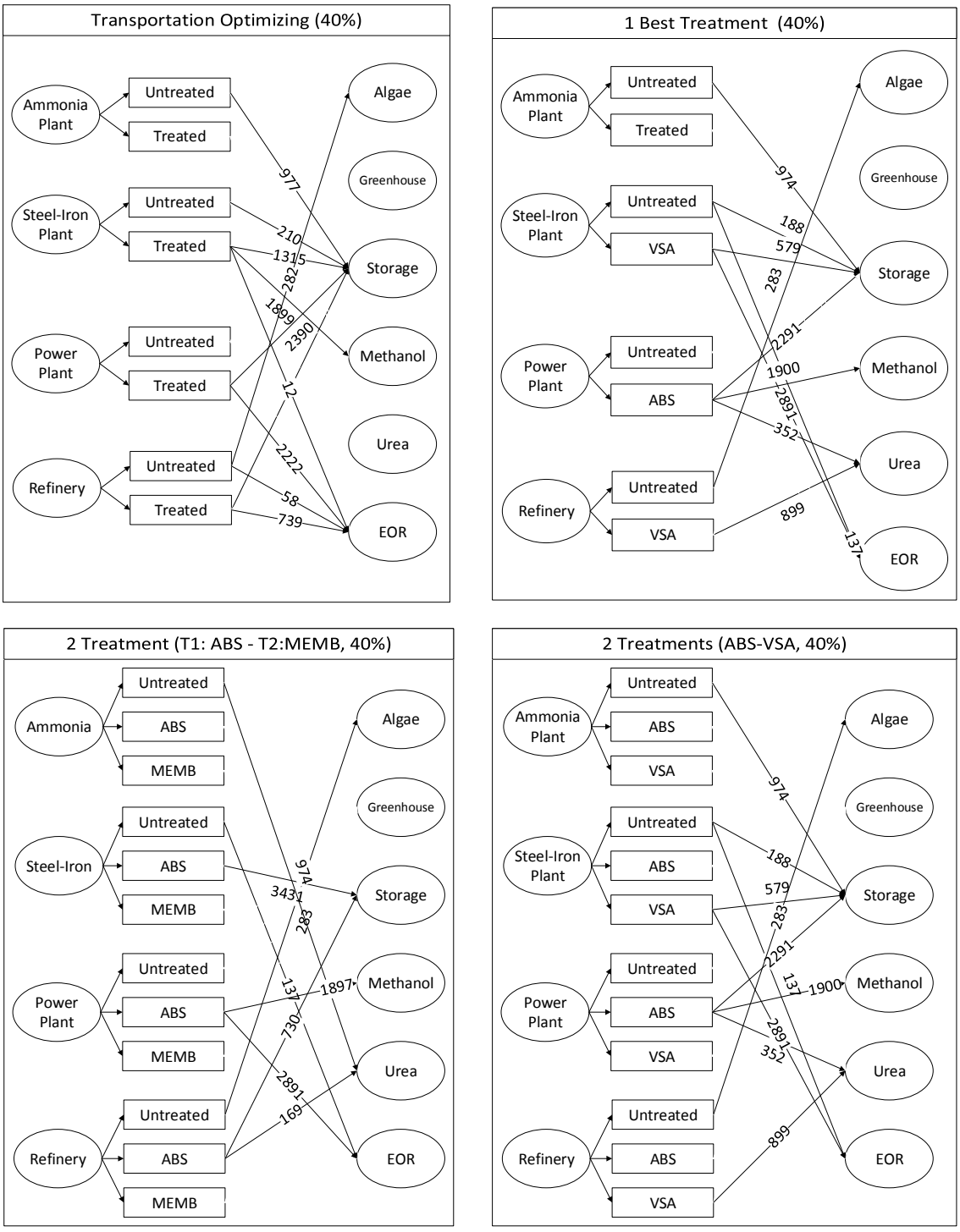

Figure 20 Carbon Allocations with Multiple Treatment Technologies for 40% Target

When the target rises to 50%, the total cost for each case is USD 89.9 million per year for case i) and ii) with ABS-VSA, USD 107 million per year for case ii) with ABS-MEMB. Capture cost for each case is USD 24.06 per ton of CO_2 net captured for case i) and ii) with ABS-VSA, and USD 28.69 per ton of CO_2 net captured for case ii) with ABS-MEMB. As indicated in 40% target scenario, due to the scale of economy, the amine absorption technology is selected and carbon dioxide stream from the steel plant is not utilized while the amine absorption technology does not have any economic advantage. The graphical allocations are shown in Figure 21, and the specific treatment costs are presented in Table 22.

Table 22 Specific Cost of Each Treatment Option in 50% Target

Transportation-optimizing design	Source / Option	Steel-Iron Plant	Power Plant	Refinery
Transportation-optimizing design	ABS	29	43	35
Case i)	ABS	-	31	-
	VSA	22	-	26
Case ii) -1	ABS	-	31	34
	MEMB	-	-	-
Case ii) -2	ABS	-	31	-
	VSA	22	-	26

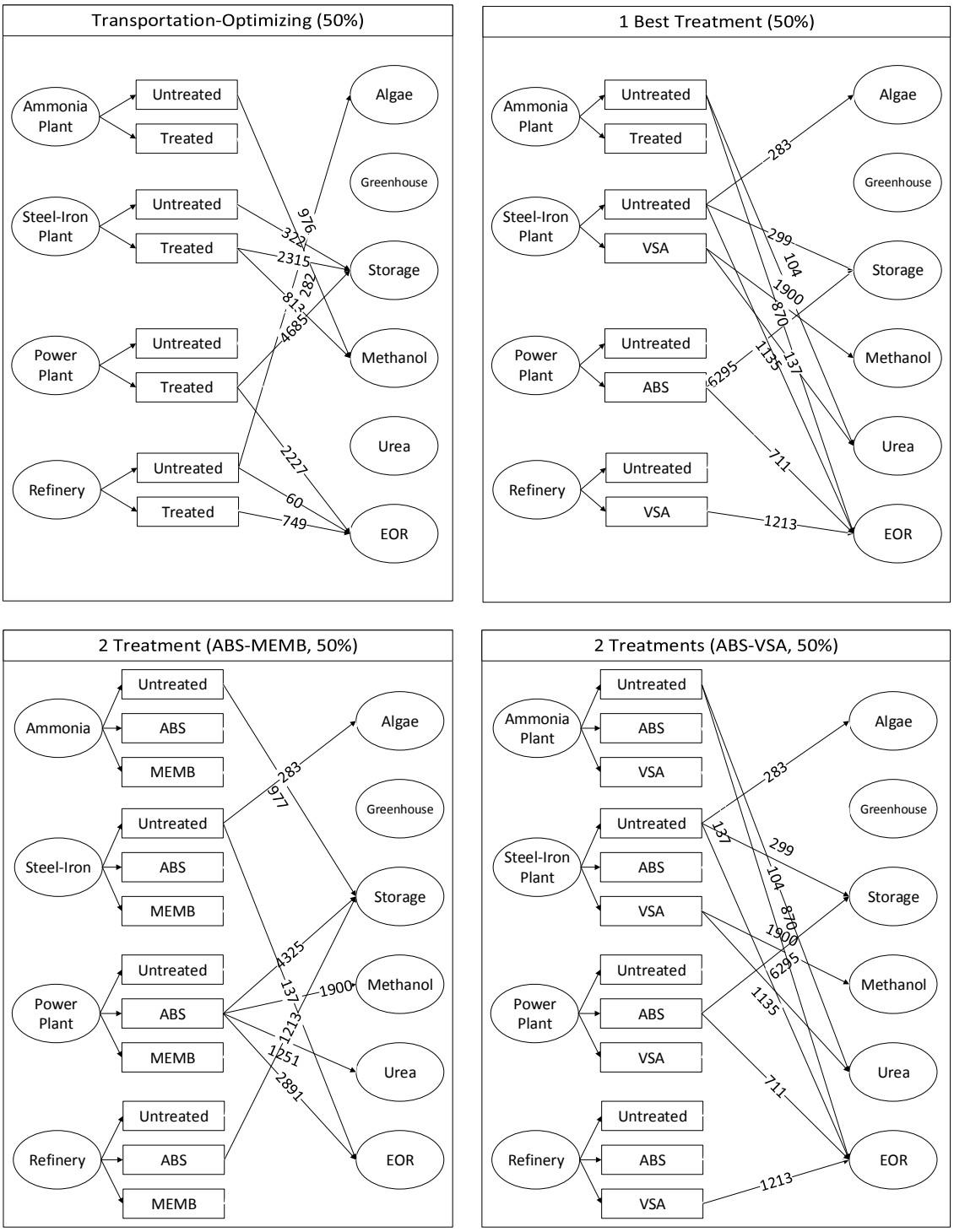

Figure 21 Carbon Allocations with Multiple Treatment Technologies for 50% Target

As expected from the analysis of Al-Mohannadi and Linke [51], reducing the treatment cost for each target significantly affects the decrease of total carbon integration cost for each carbon reduction target. More specifically, by applying various kinds of treatment technologies, each source selected the most suitable treatment process and showed less total cost than the model from Al-Mohannadi and Linke [51] with the reduction of USD 0.3 ~ 17 / t CO_2.

Also, it is possible to decrease the computation time for running the global optimization program by comparing the results of case i) (the pre-selecting suitable treatment technology for each source) with the case ii) with ABS-VSA. Results of case i) and ii) with ABS-VSA were same except the 30% reduction target scenario. However, case i) took around 2 minute and case ii) with ABS-VSA took around 5 minutes to compute the global optimized total cost. Thus, it is possible to pre-select the optimized treatment technology without complex treatment options for further carbon integration study. Additionally, over 30% of carbon reduction target, as the power plant comes into the play, the effect of reduced treatment cost increased significantly due to the economy of scale. Therefore, the key factor to implement the carbon integration into reality is the investigation of the optimized treatment cost model for each large-scale carbon emission source. For the comparison between the previous work and the result of optimizing works, the specific capture costs in Figure 22 and cost components in Figure 23 are plotted.

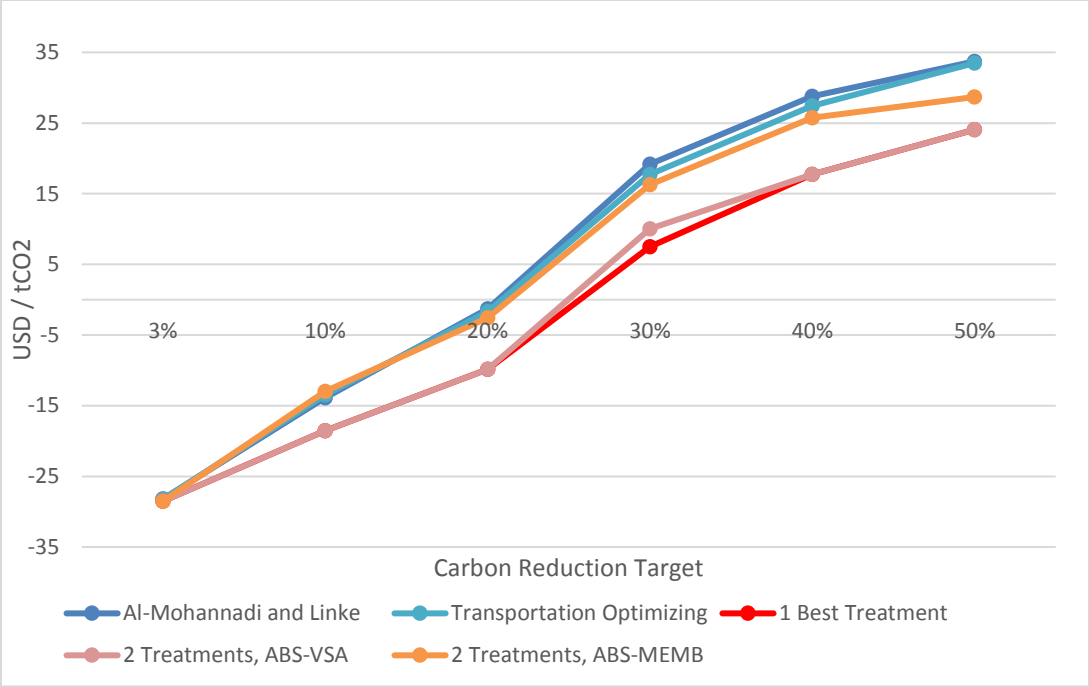

Figure 22 Carbon Integration Network Cost per ton CO2 capture (net) with Multiple Treatment Options

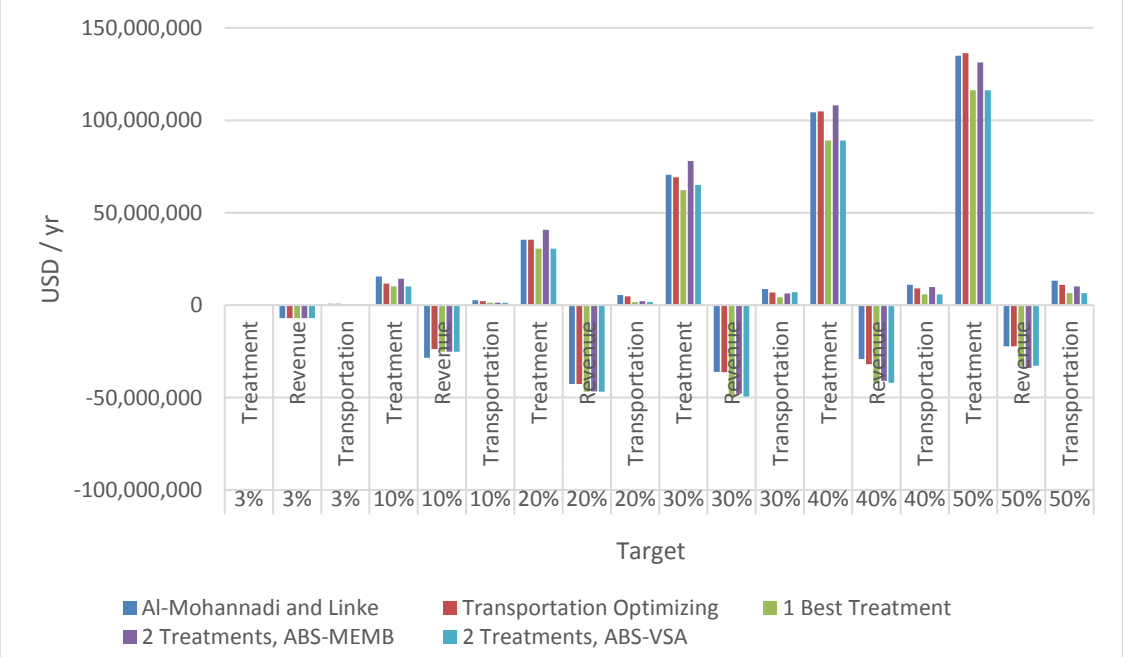

Figure 23 Comparison of Cost Components of Carbon Integration Network with Multiple Treatment Options

8. CONCLUSIONS AND FUTURE WORK

This work has presented the step-wise cost optimizations of carbon integration network for the CCUS system as following:

- Decompose the total cost into cost components in the system.
- Analyze the cost components and select the optimizable components.
- Optimize selected components and acquire new cost models.
- Simplify the carbon integration MINLP formulations to MILP formulations by substituting linear cost models for all cost components.

In this work, two cost components are mainly expected to be optimized: transportation and treatment process costs. These cost components are optimized by development and modification of new cost model coefficients, and applied to the available MINLP formulations. As a result, this work could show the following advantages:

- Optimized total cost and specific capture cost for implementing the carbon integration network for the CCUS system,
- Simple method for optimizing the transportation and treatment process,
- Prediction and selection of suitable cost models for the emission source with different composition,
- Optimized source-sink matchings which meet the carbon reduction target and the minimum cost,
- Yardstick for carbon emission industries and policy makers who are considering the implementation of the CCUS system due to the emission regulation.

For the future works, it is required to:

- Investigate the CCUS system without EOR sinks to consider many countries those pledged to reduce the carbon emission do not have EOR sites,
- Explore the more treatment options, such as cryogenic distillation,
- Include the carbon tax or government subsidy to predict the economic effect of the CCUS system,
- Develop more accurate cost models for the enhancement of this work,
- Consider the cascade or multi-stage treatment process to check the potential optimization.

REFERENCES

[1] US Department of Energy, “Overview of Greenhouse Gases,” US Department of Energy, 2016. [Online]. Available: https://www3.epa.gov/climatechange/ghgemissions/gases/co2.html. [Accessed: 23-Apr-2016].

[2] Global CCS Institute, “The Climate Change Challenge.” [Online]. Available: http://www.globalccsinstitute.com/content/climate-change-challenge. [Accessed: 23-Apr-2016].

[3] IEA Greenhouse Gas R&D Programme, “Capturing CO2,” IEA, Cheltenham, UK, 2007.

[4] UNFCCC, “Historic Paris Agreement on Climate Change,” UNFCCC, 2015. [Online]. Available: http://newsroom.unfccc.int/unfccc-newsroom/finale-cop21/.

[5] Global CCS Institute, “CO2 Degrees from Global CCS Institute.” [Online]. Available: http://co2degrees.com/. [Accessed: 23-Apr-2016].

[6] M. Campopiano and T. Henderson, “Carbon Capture and Sequestration Projects Benefit From Enhanced Oil Recovery,” The Environmetal Law Reporter, pp. 10234–10236, 2013. [Online]. Available: http://elr.info/news-analysis/43/10234/carbon-capture-and-sequestration-projects-benefit-enhanced-oil-recovery.

[7] IEAGHG, “CO2 Pipeline Infrastructure,” IEA, Cheltenham, UK, 2014.

[8] M. J. Kuby, R. S. Middleton, and J. M. Bielicki, “Analysis of Cost Savings from Networking Pipelines in CCS Infrastructure Systems,” Energy Procedia, vol. 4,

pp. 2808–2815, 2011.

[9] L. Ikeh, J. M. Race, and A. G. Aminu, “Comparing the Effects of Pipe Diameter on Flow Capacity of a CO2 Pipeline,” in Nigeria Annual International Conference and Exhibition, 2011, pp. 1–6.

[10] IPCC, IPCC Special Report on Carbon Dioxide Capture and Storage. Prepared by Working Group III of the Intergovernmental Panel on Climate Change. New York, NY, USA: Cambridge University Press, 2012.

[11] M. M. J. Knoope, A. Ramírez, and A. P. C. Faaij, “Economic Optimization of CO2 Pipeline Configurations,” Energy Procedia, vol. 37, pp. 3105–3112, 2013.

[12] N. Ghazi and J. M. Race, “Techno-economic Modelling and Analysis of CO2 Pipelines,” J. Pipeline Eng., vol. 12, no. 2, pp. 83–92, 2013.

[13] D. L. Mccollum and J. M. Ogden, “Techno-Economic Models for Carbon Dioxide Compression , Transport , and Storage Correlations for Estimating Carbon Dioxide Density and Viscosity,” Institute of Transportation Studies, University of California, 2006.

[14] M. M. J. Knoope, W. Guijt, A. Ramírez, and A. P. C. Faaij, “Improved Cost models for Optimizing CO2 Pipeline Configuration for Point-to-point Pipelines and Simple Networks,” Int. J. Greenh. Gas Control, vol. 22, pp. 25–46, 2014.

[15] Z. X. Zhang, G. X. Wang, P. Massarotto, and V. Rudolph, “Optimization of Pipeline Transport for CO2 Sequestration,” Energy Convers. Manag., vol. 47, no. 6, pp. 702–715, 2006.

[16] T. Kuramochi, A. Ramirez, W. Turkenburg, and A. Faaij, “Comparative

Assessment of CO2 Capture Technologies for Carbon-intensive Industrial Processes," Prog. Energy Combust. Sci., vol. 38, no. 1, pp. 87–112, 2012.

[17] M. Zhao, A. I. Minett, and A. T. Harris, "A Review of Techno-economic Models for the Retrofitting of Conventional Pulverised-coal Power Plants for Post-combustion Capture (PCC) of CO2," Energy Environ. Sci., pp. 25–40, 2013.

[18] A. A. Olajire, "CO2 Capture and Separation Technologies for End-of-pipe Applications – A Review," Energy, vol. 35, no. 6, pp. 2610–2628, 2010.

[19] A. J. Kidnay, W. R. Parrish, and D. G. McCartney, Fundamentals of Natural Gas Processing., CRC Press.,2006.

[20] Gas Processors Suppliers Association, GPSA Engineering Data Book, 12th ed. Tulsa, Oklahoma: Gas Processors Suppliers Association, 2004.

[21] M. T. Ho, "Techno-economic Modelling of CO2 Capture Systems for Australian Industrial Sources," University of New South Wales, 2007.

[22] N. MacDowell, N. Florin, A. Buchard, J. Hallett, A. Galindo, G. Jackson, C. S. Adjiman, C. K. Williams, N. Shah, and P. Fennell, "An Overview of CO2 Capture Technologies," Energy Environ. Sci., vol. 3, no. 11, p. 1645, 2010.

[23] M. Gupta, I. Coyle, and K. Thambimuthu, "CO2 Capture Technologies and Opportunities in Canada.," in Strawman Document for CO2 capture and Storage (CC&S) Technology Roadmap, 2003, no. September, pp. 1–15.

[24] A. Samanta, A. Zhao, G. K. H. Shimizu, P. Sarkar, and R. Gupta, "Post-combustion CO2 Capture Using Solid Sorbents: A Review," Ind. Eng. Chem. Res., vol. 51, no. 4, pp. 1438–1463, 2012.

[25] A. Raksajati, M. T. Ho, and D. E. Wiley, “Reducing the Cost of CO 2 Capture from Flue Gases Using Aqueous Chemical Absorption,” Ind. Eng. Chem. Res., vol. 52, pp. 16887–16901, 2013.

[26] W. Ho and K. Sirkar, Membrane Handbook., Springer Science-Business Inc., 1992.

[27] X. Zhang, X. He, and T. Gundersen, “Post-combustion Carbon Capture with a Gas Separation Membrane : Parametric Study , Capture Cost , and Exergy Analysis,” Energy Fuels, vol. 27, pp. 4137–4149, 2013.

[28] P. Shao, M. M. Dal-Cin, M. D. Guiver, and A. Kumar, “Simulation of Membrane-based CO2 Capture in a Coal-fired Power Plant,” J. Memb. Sci., vol. 427, pp. 451–459, 2013.

[29] V. Duraccio, M. G. Gnoni, and V. Elia, “Carbon Capture and Reuse in an Industrial District: A Technical and Economic Feasibility Study,” J. CO2 Util., vol. 10, pp. 23–29, 2015.

[30] T. C. Merkel, H. Lin, X. Wei, and R. Baker, “Power Plant Post-combustion Carbon Dioxide Capture : An Opportunity for Membranes,” J. Memb. Sci., vol. 359, no. 1–2, pp. 126–139, 2010.

[31] H. Zhai and E. S. Rubin, “The Effects of Membrane-based CO2 Capture System on Pulverized Coal Power Plant Performance and Cost,” Energy Procedia, vol. 37, pp. 1117–1124, 2013.

[32] C. A. Scholes, M. T. Ho, D. E. Wiley, G. W. Stevens, and S. E. Kentish, “Cost Competitive Membrane—Cryogenic Post-combustion Carbon Capture,” Int. J.

Greenh. Gas Control, vol. 17, pp. 341–348, 2013.

[33] A. Agarwal, "Advanced Strategies for Optimal Design and Operation of Pressure Swing Adsorption Processes," Carnegie Mellon University, 2010.

[34] D. M. Ruthven, Principles of Adsorption and Adsorption Processes., John Wiley and Sons, 1984.

[35] C. J. Geankoplis, Transport Processes and Unit Operations, 3rd ed. Pearson Education Limited, 1993.

[36] D. M. Ruthven, S. Farooq, and K. S. Knaebel, Pressure Swing Adsorption. WILEY-VCH, 1993.

[37] J. Tóth, Adsorption: Theory, Modeling, and Analysis., Marcel Dekker Inc., 2002.

[38] B. K. Dutta, Principles of Mass Transfer and Separation Processes. Rajkamal Electric Press, 2009.

[39] J. Zhang, P. A. Webley, and P. Xiao, "Effect of Process Parameters on Power Requirements of Vacuum Swing Adsorption Technology for CO2 Capture from Flue Gas," Energy Convers. Manag., vol. 49, no. 2, pp. 346–356, 2008.

[40] Z. Liu, C. A. Grande, P. Li, J. Yu, and A. E. Rodrigues, "Multi-bed Vacuum Pressure Swing Adsorption for Carbon Dioxide Capture from Flue Gas," Sep. Purif. Technol., vol. 81, no. 3, pp. 307–317, 2011.

[41] J. A. Delgado, M. A. Uguina, J. L. Sotelo, V. I. Agueda, A. Sanz, and P. Gomez, "Numerical Analysis of CO2 Concentration and Recovery from Flue Gas by a Novel Vacuum Swing Adsorption Cycle," Comput. Chem. Eng., vol. 35, no. 6, pp. 1010–1019, 2011.

[42] J. Ling, A. Ntiamoah, P. Xiao, P. A. Webley, and Y. Zhai, “Effects of feed gas concentration, temperature and process parameters on vacuum swing adsorption performance for CO2 capture,” Chem. Eng. J., vol. 265, pp. 47–57, 2015.

[43] P. Linke and A. Kokossis, “Process Synthesis/Integration,” in Re-engineering the Chemical Processing Plant : Process Intensification, A. Stankiewicz and J. A. Moulijn, Eds. M. Dekker, 2004, pp. 385–423.

[44] M. M. El-Halwagi, Sustainable Design through Process Integration : Fundamentals and Applications to Industrial Pollution Prevention, Resource Conservation, and Profitability Enhancement. 2012.

[45] J. A. R. Diamante, R. R. Tan, D. C. Y. Foo, D. K. S. Ng, K. B. Aviso, and S. Bandyopadhyay, “A Graphical Approach for Pinch-Based Source–Sink Matching and Sensitivity Analysis in Carbon Capture and Storage Systems,” Ind. Eng. Chem. Res., vol. 52, no. 22, pp. 7211–7222, 2013.

[46] R. E. H. Ooi, D. C. Y. Foo, D. K. S. Ng, and R. R. Tan, “Planning of Carbon Capture and Storage with Pinch analysis Techniques,” Chem. Eng. Res. Des., vol. 91, no. 12, pp. 2721–2731, 2013.

[47] D. C. Y. Foo, R. R. Tan, and D. K. S. Ng, “Carbon and Footprint-constrained Energy Planning Using Cascade Analysis Technique,” Energy, vol. 33, pp. 1480–1488, 2008.

[48] Y.-J. He, Y. Zhang, Z.-F. Ma, N. V. Sahinidis, R. R. Tan, and D. C. Y. Foo, “Optimal Source–Sink Matching in Carbon Capture and Storage Systems under Uncertainty,” Ind. Eng. Chem. Res., vol. 53, no. 2, pp. 778–785, 2014.

[49] Z. Zheng, D. Gao, L. Ma, Z. Li, and W. Ni, “CO2 Capture and Sequestration Source-Sink Match Optimization in Jing-Jin-Ji Region of China,” Front. Energy Power Eng. China, vol. 3, no. 3, pp. 359–368, 2009.

[50] R. S. Middleton, “A New Optimization Approach to Energy Network Modeling : Anthropogenic CO2 Capture Coupled with Enhanced Oil Recovery,” Int. J. energy Res., vol. 37, no. December 2012, pp. 1794–1810, 2013.

[51] D. M. Al-Mohannadi and P. Linke, “On the Systematic Carbon Integration of Industrial Parks for Climate Footprint Reduction,” J. Clean. Prod., vol. 112, pp. 4053–4064, 2016.

[52] M. M. F. Hasan, R. C. Baliban, J. A. Elia, and C. A. Floudas, “Modeling, Simulation, and Optimization of Postcombustion CO2 Capture for Variable Feed Concentration and Flow Rate. 2. Pressure Swing Adsorption and Vacuum Swing Adsorption Processes,” Ind. Eng. Chem. Res., vol. 51, no. 48, pp. 15665–15682, 2012.

[53] M. M. F. Hasan, R. C. Baliban, J. Elia, and C. A. Floudas, “Modeling, Simulation, and Optimization of Postcombustion CO2 Capture for Variable Feed Concentration and Flow Rate. 1. Chemical Absorption and Membrane Processes,” Ind. Eng. Chem. Res., vol. 51, pp. 15642–15664, 2012.

[54] American National Standards Institute, “ANSI B36.19: Welded and Seamless Wrought Steel Pipe,” vol. 552, no. 1, 2013.

[55] R. K. Sinnott and G. Towler, Chemical Engineering Design., Butterworth-Heinemann, 2013.

[56] S. M. Walas, Chemical Process Equipment Selection and Design., Butterworth-Heinemann, 1990.

[57] P. S, R. H. Perry, D. W. Green, and J. O. Maloney, Chemical Engineers ' Handbook, Seventh Edit., McGraw Hill Professional,. 1997.

[58] S. I. Sandler, Chemical, Biochemical, and Engineering Thermodynamics, John Wiley & Sons, Inc. 2006.

[59] X. GAO, L. MENG, and W. CHANG, "Study on the Density of Supercritical CO2 with State Equation," Appl. Mech. Mater., vol. 556–562, pp. 3749–3751, 2014.

[60] American National Standards Institute, ANSI B36.19: Welded and Seamless Wrought Steel Pipe. American National Standard Institute, 2013.

[61] A. Fenghour, W. A. Wakeham, and V. Vesovic, "The Viscosity of Carbon Dioxide," Proc. R. Soc. A Math. Phys. Eng. Sci., vol. 87, no. 1998, pp. 48–61, 1998.

[62] A. K. Coker, Ludwig's Applied Process Design for Chemical and Petrochemical Plants. Fourth Edit., Butterworth-Heinemann, 1995.

[63] M. Mohitpour, S. Golshan, and A. Murray, Pipeline Design & Construction: A Practical Approach. New York: The American Society of Mechanical Engineers, 2000.

[64] Lindo Systems, "What's Best! - Excel Add-In for Linear, Nonlinear, and Integer Modeling and Optimization." [Online]. Available: http://www.lindo.com/index.php?option=com_content&view=article&id=3&Item

id=11. [Accessed: 30-Apr-2016].

[65] UNFCCC, “Framework Convention on Climate Change Compilation of Economy-wide Emission Reduction Targets to Convention,” UN Office, Geneva, Swiss., 2011.

[66] J. Sumner, L. Bird, and H. Smith, “Carbon Taxes : A Review of Experience and Policy Design Considerations Carbon Taxes,” National Renewable Energy Laboratory., 2009.

[67] Carbon Tax Center, “Where Carbon is Taxed,” 2015. [Online]. Available: http://www.carbontax.org/where-carbon-is-taxed/. [Accessed: 23-Apr-2016].

[68] G. Farrar, “Nelson-Farrar Quarterly Costimating Indexes for selected equipment items,” Oil Gas J., 2015, 2015. [Online]. Available: http://www.ogj.com/articles/print/volume-113/issue-7/processing/nelson-farrar-quarterly-costimatin. [Accessed: 19-May-2016].

APPENDIX A

In this section, the CO2 exchange streams of every work result (Result of Al-Mohannadi and Linke [51], the transportation-optimizing work, multiple treatment option case i), case ii) with ABS – MEMB and case ii) with ABS – VSA are presented. The treated source streams are indicated by abbreviation T., and the untreated sources are displayed with abbreviation UT.

A1. 3% of Carbon Reduction Target

Table 23 CO_2 Exchange of Transportation-optimizing Work for 3% Target

tCO_2/d	Algae	Greenhouse	Saline Storage	Methanol Plant	Urea Plant	EOR
Ammonia Plant, T	0	0	0	0	0	1
Steel-Iron Plant, T	0	0	0	0	0	0
Power Plant, T	0	0	0	0	0	0
Refinery, T	0	0	0	0	0	0
Ammonia Plant, UT	0	0	0	0	0	639
Steel-Iron Plant, UT	0	0	0	0	0	0
Power Plant, UT	0	0	0	0	0	0
Refinery, UT	0	0	0	0	0	0

Table 24 CO_2 Exchange of Case i) for 3% Target

tCO_2/d	Algae	Greenhouse	Saline Storage	Methanol Plant	Urea Plant	EOR
Ammonia Plant, T	0	0	0	0	0	0
Steel-Iron Plant, T	0	0	0	0	0	0
Power Plant, T	0	0	0	0	0	0
Refinery, T	0	0	0	0	0	0
Ammonia Plant, UT	0	0	0	0	0	640
Steel-Iron Plant, UT	0	0	0	0	0	0
Power Plant, UT	0	0	0	0	0	0
Refinery, UT	0	0	0	0	0	0

Table 25 CO_2 Exchange of Case ii) with ABS-MEMB for 3% Target

tCO_2/d	Algae	Greenhouse	Saline Storage	Methanol Plant	Urea Plant	EOR
Ammonia Plant, T	0	0	0	0	0	0
Steel-Iron Plant, T	0	0	0	0	0	0
Power Plant, T	0	0	0	0	0	0
Refinery, T	0	0	0	0	0	0
Ammonia Plant, UT	0	0	0	0	0	640
Steel-Iron Plant, UT	0	0	0	0	0	0
Power Plant, UT	0	0	0	0	0	0
Refinery, UT	0	0	0	0	0	0

Table 26 CO_2 Exchange of Case ii) with ABS-VSA for 3% Target

tCO_2/d	Algae	Greenhouse	Saline Storage	Methanol Plant	Urea Plant	EOR
Ammonia Plant, T	0	0	0	0	0	0
Steel-Iron Plant, T	0	0	0	0	0	0
Power Plant, T	0	0	0	0	0	0
Refinery, T	0	0	0	0	0	0
Ammonia Plant, UT	0	0	0	0	0	640
Steel-Iron Plant, UT	0	0	0	0	0	0
Power Plant, UT	0	0	0	0	0	0
Refinery, UT	0	0	0	0	0	0

A2. 10% of Carbon Reduction Target

Table 27 CO_2 Exchange of Transportation-optimizing Work for 10% Target

tCO_2/d	Algae	Greenhouse	Saline Storage	Methanol Plant	Urea Plant	EOR
Ammonia Plant, T	0	0	0	0	0	1
Steel-Iron Plant, T	0	0	0	0	0	1216
Power Plant, T	0	0	0	0	0	0
Refinery, T	0	0	0	0	0	0
Ammonia Plant, UT	0	0	0	0	0	976
Steel-Iron Plant, UT	0	0	0	0	0	109
Power Plant, UT	0	0	0	0	0	0
Refinery, UT	0	0	0	0	0	0

Table 28 CO_2 Exchange of Case i) for 10% Target

tCO_2/d	Algae	Greenhouse	Saline Storage	Methanol Plant	Urea Plant	EOR
Ammonia Plant, T	0	0	0	0	0	0
Steel-Iron Plant, T	0	0	0	0	0	1216
Power Plant, T	0	0	0	0	0	3
Refinery, T	0	0	0	0	0	0
Ammonia Plant, UT	0	0	0	0	0	976
Steel-Iron Plant, UT	0	0	0	0	0	109
Power Plant, UT	0	0	0	0	0	0
Refinery, UT	0	0	0	0	0	0

Table 29 CO_2 Exchange of Case ii) with ABS-MEMB for 10% Target

tCO_2/d	Algae	Greenhouse	Saline Storage	Methanol Plant	Urea Plant	EOR
Ammonia Plant, T	0	0	0	0	0	0
Steel-Iron Plant, T	0	0	0	0	0	1216
Power Plant, T	0	0	0	0	0	0
Refinery, T	0	0	0	0	0	0
Ammonia Plant, UT	0	0	0	0	0	977
Steel-Iron Plant, UT	0	0	0	0	0	109
Power Plant, UT	0	0	0	0	0	0
Refinery, UT	0	0	0	0	0	0

Table 30 CO_2 Exchange of Case ii) with ABS-VSA for 10% Target

tCO_2/d	Algae	Greenhouse	Saline Storage	Methanol Plant	Urea Plant	EOR
Ammonia Plant, T	0	0	0	0	0	0
Steel-Iron Plant, T	0	0	0	0	0	1214
Power Plant, T	0	0	0	0	0	0
Refinery, T	0	0	0	0	0	0
Ammonia Plant, UT	0	0	0	0	0	977
Steel-Iron Plant, UT	0	0	0	0	0	109
Power Plant, UT	0	0	0	0	0	0
Refinery, UT	0	0	0	0	0	0

A3. 20% of Carbon Reduction Target

Table 31 CO_2 Exchange of Transportation-optimizing Work for 20% Target

tCO_2/d	Algae	Greenhouse	Saline Storage	Methanol Plant	Urea Plant	EOR
Ammonia Plant, T	0	0	0	1	0	0
Steel-Iron Plant, T	0	0	0	761	0	2554
Power Plant, T	0	0	0	0	0	0
Refinery, T	1	0	0	0	0	338
Ammonia Plant, UT	0	0	0	971	0	0
Steel-Iron Plant, UT	0	0	0	1	0	135
Power Plant, UT	0	0	0	0	0	0
Refinery, UT	282	0	0	0	0	1

Table 32 CO_2 Exchange of Case i) for 20% Target

tCO_2/d	Algae	Greenhouse	Saline Storage	Methanol Plant	Urea Plant	EOR
Ammonia Plant, T	0	0	0	0	0	0
Steel-Iron Plant, T	0	0	0	559	0	2891
Power Plant, T	0	0	0	0	0	0
Refinery, T	0	0	0	257	0	0
Ammonia Plant, UT	0	0	0	977	0	0
Steel-Iron Plant, UT	210	0	0	0	0	137
Power Plant, UT	0	0	0	0	0	0
Refinery, UT	0	0	0	0	0	0

Table 33 CO_2 Exchange of Case ii) with ABS-MEMB for 20% Target

tCO_2/d	Algae	Greenhouse	Saline Storage	Methanol Plant	Urea Plant	EOR
Ammonia Plant, T	0	0	0	0	0	0
Steel-Iron Plant, T	0	0	0	791	0	2891
Power Plant, T	0	0	0	0	0	0
Refinery, T	0	0	0	0	0	0
Ammonia Plant, UT	0	0	0	977	0	0
Steel-Iron Plant, UT	0	0	0	0	0	137
Power Plant, UT	0	0	0	0	0	0
Refinery, UT	244	0	0	0	0	0

Table 34 CO_2 Exchange of Case ii) with ABS-VSA for 20% Target

tCO_2/d	Algae	Greenhouse	Saline Storage	Methanol Plant	Urea Plant	EOR
Ammonia Plant, T	0	0	0	3	0	0
Steel-Iron Plant, T	0	0	0	558	0	2891
Power Plant, T	0	0	0	0	0	0
Refinery, T	0	0	0	257	0	0
Ammonia Plant, UT	0	0	0	977	0	0
Steel-Iron Plant, UT	210	0	0	0	0	137
Power Plant, UT	0	0	0	0	0	0
Refinery, UT	0	0	0	0	0	0

A4. 30% of Carbon Reduction Target

Table 35 CO_2 Exchange of Transportation-optimizing Work for 30% Target

tCO_2/d	Algae	Greenhouse	Saline Storage	Methanol Plant	Urea Plant	EOR
Ammonia Plant, T	0	0	11	1	0	0
Steel-Iron Plant, T	0	6	379	837	0	2084
Power Plant, T	0	0	2007	0	0	0
Refinery, T	1	0	0	0	0	808
Ammonia Plant, UT	0	0	10	955	0	0
Steel-Iron Plant, UT	0	4	4	1	0	135
Power Plant, UT	0	0	1	0	0	0
Refinery, UT	282	0	0	0	0	1

Table 36 CO_2 Exchange of Case i) for 30% Target

tCO_2/d	Algae	Greenhouse	Saline Storage	Methanol Plant	Urea Plant	EOR
Ammonia Plant, T	0	0	0	0	0	0
Steel-Iron Plant, T	0	0	0	1900	1251	446
Power Plant, T	0	0	526	0	0	1546
Refinery, T	0	0	0	0	0	899
Ammonia Plant, UT	0	0	977	0	0	0
Steel-Iron Plant, UT	0	0	77	0	0	137
Power Plant, UT	0	0	0	0	0	0
Refinery, UT	283	0	0	0	0	0

Table 37 CO_2 Exchange of Case ii) with ABS-MEMB for 30% Target

tCO_2/d	Algae	Greenhouse	Saline Storage	Methanol Plant	Urea Plant	EOR
Ammonia Plant, T	0	0	0	0	0	0
Steel-Iron Plant, T	0	0	0	0	0	0
Power Plant, T	0	0	1887	814	38	2891
Refinery, T	0	0	0	0	1213	0
Ammonia Plant, UT	0	0	0	977	0	0
Steel-Iron Plant, UT	0	0	0	0	0	137
Power Plant, UT	0	0	0	0	0	0
Refinery, UT	0	0	0	0	0	0

Table 38 CO_2 Exchange of Case ii) with ABS-VSA for 30% Target

tCO_2/d	Algae	Greenhouse	Saline Storage	Methanol Plant	Urea Plant	EOR
Ammonia Plant, T	0	0	0	3	0	0
Steel-Iron Plant, T	0	0	0	0	1248	2129
Power Plant, T	0	0	1549	0	0	666
Refinery, T	0	0	0	1201	0	0
Ammonia Plant, UT	0	265	0	629	0	83
Steel-Iron Plant, UT	275	0	0	0	0	137
Power Plant, UT	0	0	0	0	0	0
Refinery, UT	0	0	0	0	0	0

A5. 40% of Carbon Reduction Target

Table 39 CO_2 Exchange of Transportation-optimizing Work for 40% Target

tCO_2/d	Algae	Greenhouse	Saline Storage	Methanol Plant	Urea Plant	EOR
Ammonia Plant, T	0	0	967	0	0	0
Steel-Iron Plant, T	0	6	1315	1899	0	12
Power Plant, T	0	0	2390	0	0	2222
Refinery, T	1	0	11	0	0	739
Ammonia Plant, UT	0	0	10	0	0	0
Steel-Iron Plant, UT	0	4	210	1	0	4.4
Power Plant, UT	0	0	1	0	0	1
Refinery, UT	282	0	1	0	0	58

Table 40 CO_2 Exchange of Case i) for 40% Target

tCO_2/d	Algae	Greenhouse	Saline Storage	Methanol Plant	Urea Plant	EOR
Ammonia Plant, T	0	0	0	0	0	0
Steel-Iron Plant, T	0	3	579	0	0	2891
Power Plant, T	0	0	2291	1900	352	0
Refinery, T	0	0	0	0	899	0
Ammonia Plant, UT	0	3	974	0	0	0
Steel-Iron Plant, UT	0	0	188	0	0	137
Power Plant, UT	0	0	0	0	0	0
Refinery, UT	283	0	0	0	0	0

Table 41 CO_2 Exchange of Case ii) with ABS-MEMB for 40% Target

tCO_2/d	Algae	Greenhouse	Saline Storage	Methanol Plant	Urea Plant	EOR
Ammonia Plant, T	0	0	0	0	0	0
Steel-Iron Plant, T	0	0	3431	0	0	0
Power Plant, T	0	0	0	1897	0	2891
Refinery, T	0	0	730	0	169	0
Ammonia Plant, UT	0	0	0	3	974	0
Steel-Iron Plant, UT	0	0	0	0	0	137
Power Plant, UT	0	0	0	0	0	0
Refinery, UT	283	0	0	0	0	0

Table 42 CO_2 Exchange of Case ii) with ABS-VSA for 40% Target

tCO_2/d	Algae	Greenhouse	Saline Storage	Methanol Plant	Urea Plant	EOR
Ammonia Plant, T	0	3	579	0	0	2891
Steel-Iron Plant, T	0	0	2291	1900	352	0
Power Plant, T	0	0	0	0	899	0
Refinery, T	0	3	974	0	0	0
Ammonia Plant, UT	0	0	188	0	0	137
Steel-Iron Plant, UT	0	0	0	0	0	0
Power Plant, UT	283	0	0	0	0	0
Refinery, UT	0	3	579	0	0	2891

A6. 50% of Carbon Reduction Target

Table 43 CO_2 Exchange of Transportation-optimizing Work for 50% Target

tCO_2/d	Algae	Greenhouse	Saline Storage	Methanol Plant	Urea Plant	EOR
Ammonia Plant, T	0	0	0	1	0	0
Steel-Iron Plant, T	0	0	2315	813	0	0
Power Plant, T	0	0	4685	0	0	2227
Refinery, T	1	0	0	0	0	749
Ammonia Plant, UT	0	0	0	976	0	0
Steel-Iron Plant, UT	0	0	322	1	0	0
Power Plant, UT	0	0	1	0	0	1
Refinery, UT	282	0	0	0	0	60

Table 44 CO_2 Exchange of Case i) for 50% Target

tCO_2/d	Algae	Greenhouse	Saline Storage	Methanol Plant	Urea Plant	EOR
Ammonia Plant, T	0	0	0	0	0	0
Steel-Iron Plant, T	0	0	0	1900	1135	0
Power Plant, T	0	0	6295	0	0	711
Refinery, T	0	0	0	0	0	1213
Ammonia Plant, UT	0	3	0	0	104	870
Steel-Iron Plant, UT	283	0	299	0	0	137
Power Plant, UT	0	0	0	0	0	0
Refinery, UT	0	0	0	0	0	0

Table 45 CO_2 Exchange of Case ii) with ABS-MEMB for 50% Target

tCO_2/d	Algae	Greenhouse	Saline Storage	Methanol Plant	Urea Plant	EOR
Ammonia Plant, T	0	0	0	3	0	0
Steel-Iron Plant, T	0	0	0	0	0	0
Power Plant, T	0	0	4325	1900	1251	2891
Refinery, T	0	0	1213	0	0	0
Ammonia Plant, UT	0	0	977	0	0	0
Steel-Iron Plant, UT	283	0	0	0	0	137
Power Plant, UT	0	0	0	0	0	0
Refinery, UT	0	0	0	0	0	0

Table 46 CO_2 Exchange of Case ii) with ABS-VSA for 50% Target

tCO_2/d	Algae	Greenhouse	Saline Storage	Methanol Plant	Urea Plant	EOR
Ammonia Plant, T	0	0	0	0	0	0
Steel-Iron Plant, T	0	0	0	1900	1135	0
Power Plant, T	0	0	6295	0	0	711
Refinery, T	0	0	0	0	0	1213
Ammonia Plant, UT	0	3	0	0	104	870
Steel-Iron Plant, UT	283	0	299	0	0	137
Power Plant, UT	0	0	0	0	0	0
Refinery, UT	0	0	0	0	0	0